EXPLOITING ENDOGENOUS NITRIC OXIDE TO IMPROVE

THE HAEMOCOMPATIBILITY OF BIOMATERIALS

By

XUNBAO DUAN

Bachelor of Engineering
Tianjin University
Tianjin, P. R. China
July, 1992

Master of Science
Tsinghua University
Beijing, P. R. China
July, 1995

Submitted to the Faculty of the
Graduate College of the
Oklahoma State University
in partial fulfillment of
the requirements for
the Degree of
DOCTOR OF PHILOSOPHY
May, 2001

EXPLOITING ENDOGENOUS NITRIC OXIDE TO IMPROVE

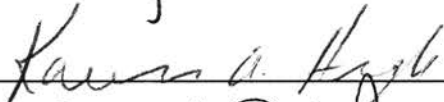THE HAEMOCOMPATIBILITY OF BIOMATERIALS

Thesis Approved:

Randy S. Lewis
Thesis Advisor

Warren T. Ford

Gary L. Foutch

Karen A. High

Arland H. Johannes

Alfred Carlozzi
Dean of the Graduate College

ACKNOWLEDGEMENTS

TABLE OF CONTENTS

LIST OF TABLES

LIST OF FIGURES

vii

NOMENCLATURE

A	The area of L-cysteine-modified polymer
ACD	Acid-citric acid-dextrose used as an anticoagulant
ADP	Adenosine diphosphate
albSNO	S-nitroso-bovine serum albumin or S-nitroso-human serum albumin
AlbSNO	S-nitroso-human serum albumin
cAMP	Cyclic adenosine monophosphate
APC	Activated protein C
APTES	3-aminopropyltriethoxysilane
ATIII	Antithrombin III
ATP	Adenosine triphosphate
BCA	Bicinchoninic acid
BSA	Bovine serum albumin
BSANO	S-nitroso-bovine serum albumin
cGMP	Cyclic guanosine 3' 5'-monophosphate
CySH	L-cysteine
CySNO	S-nitroso-L-cysteine
DAG	Diacylglycerol
DTPA	Diethylenetriaminepentaacetic acid
EDRF	Endothelium-derived relaxing factor

GA	Glutaraldehyde
GP	Glycoprotein
GSH	Glutathione
GSNO	S-nitroso-glutathione
GTP	Guanosine 5'-triphosphate
HSA	Human serum albumin
5-IAF	5-Iodoacetamidofluorescein
IP_3	Inositol 1,4,5-triphosphate
K	Equilibrium constant for transnitrosation
K_D	Distribution coefficient
K_{BSA}	Rate constant for BSANO self deomposition
k_{CYS}	Rate constant for CySNO self deomposition
k_f	Forward rate constant for transnitrosation
k_v	Reverse rate constant for transnitrosation
LB	Langmuir-Blodgett
N_A	Avagadro constant
PAF	Platelet-activating factor
PBS	Phosphate buffer saline
PET	Polyethylene terephthalate
PET-Cys	L-cysteine-modified polyethylene terephthalate
PG	Prostaglandins
PIP_2	Phosphatidylinositol 4,5-bisphosphate
PS	Phosphatidylserine

PU	Polyurethane
PU-Cys	L-cysteine-modified polyurethane
RSFG	Radio frequency glow discharges
RSH	Thiols
RSSR	Disulfide
RSNO	S-nitrosothiol
SAM	Self-assembled monolayer
SGC	Soluble guanylate cyclase
SMA	Surface-modifying additives
TM	Thrombomodulin
t-PA	Tissue-type plasminogen activator
TxA_2	Thromboxane A_2
u-PA	Urokinase-type plasminogen activator
V	Volume of liquid phase for transnitrosation
V_e	Elution volume of a particular solute
V_o	Void volume of gel bed
V_t	Volume of gel bed used in gel filtration
V_x	Volume of the gel beads
vWF	von Willebrand factor

CHAPTER 1

INTRODUCTION

Biomaterials are defined as nonviable materials used as medical devices that interact with biological systems [Williams, 1987]. Biomaterials are widely used to resolve pathologies that cannot be corrected either by the natural healing process or traditional surgery. The total sale of medical devices incorporating biomaterials currently exceeds $100 billion in the U. S. [Peppas and Langer, 1994] and there is a far greater potential for profits to increase since the artificial organs and tissues formed by tissue engineering technology are promising in clinical applications [Langer, 2000]. Biomaterials consist of a variety of synthetic materials including metals, ceramics, glasses, carbons, composite materials, and polymers. Polymeric biomaterials play a dominant role in medical devices such as blood oxygenators and filters, kidney dialyzers, heart valves, and vascular grafts [Wise et al., 1996]. Although these devices, as shown in Table 1.1, have been successfully used in patients for many years, the haemocompatibility (blood compatibility) of the polymers used in these devices has been a constant concern in biomaterials science.

A haemocompatible device is one that functions in contact with blood without inducing adverse reactions, such as blood clots. However, to date, the performance of blood-contacting medical devices are still complicated with platelet adhesion and aggregation, formation of thrombus, and shedding of emboli (detached thrombus) [Ratner

1

et al., 1996; Mowery *et al.,* 2000; Schoenfisch *et al.,* 2000]. Such complications can compromise the device function, such as the delivery of blood through artificial blood vessels, gas exchange through oxygenators, or the removal of metabolic waste products through dialysis membranes. Furthermore, the complications may produce potential side effects on patients, which include:

- Severe bleeding from platelet depletion due to platelet adhesion and aggregation on the device.

- Life-threatening stroke due to emboli (detached thrombi) formation.

- and /or ischemia (lack of oxygen) and dysfunction of downstream endothelial cells which may be further implicated in vasospasm [Vallance, 1989], hypertension, and inflammation [Traub and Berk, 1998].

Thus, the haemocompatibility of the current blood-contacting polymers needs to be further optimized.

Table 1.1

The market size of medical devices involving blood-contacting polymers (per year) [a]

Medical Devices	Market Size
Vascular grafts	250,000 [c]
Heart valves	45,000 [b]
Pacemakers	460,000 [b]
Blood bags	30,000,000 [c]
Oxygenators	500,000 [c]
Renal dialyzers	16,000,000 [c]
Catheters	200,000,000 [c]

[a] Reproduced in part from Ratner *et al.* (1996).
[b] 1990 for U. S.
[c] 1981 for western countries and Japan.

At present, systemic administration of heparin is widely used to reduce potential clotting activation in extracorporeal polymer-based circuits [Graves *et al.*, 1996]. The use of heparin has advantages since it is inexpensive and rapidly neutralized by the administration of protamine [Muntean, 1999]. Unfortunately, heparin has no inhibitory effect on platelet adhesion, and platelet loss is usually observed in most heparin applications. Additionally, a complex of heparin formed with platelet factor 4 (PF4) can induce thrombocytopenia (patient's platelet count in blood is less than normal $150 - 400 \times 10^6$ per ml) that may lead to massive thrombembolisms [Mammen, 1999]. Thus, the risk of bleeding potentially exists during heparin anticoagulation due to the loss of platelets and other clotting factors. Other antithrombogenic compounds (prostacyclin, glycoprotein IIb/IIIa receptor antagonists, and adenosine diphosphate receptor inhibitors) are still under investigation for minimizing platelet adhesion [Muntean, 1999].

In the past decades, numerous investigations concentrated on surface modification to enhance the haemocompatibility of blood-contacting polymers [Ratner and Castner, 1997]. Modifications included grafting anticoagulants such as heparin [Han *et al.*, 1989, Kang *et al.*, 1996] and hirudin [Seifert *et al.*, 1997], increasing the surface hydrophilicity via poly(ethyleneoxide) [Morra *et al.*, 1993; Litauszki et al., 1997], and passivation by coupling albumin to the surface [Amiji and Park, 1992; de Queiro *et al.*, 1997]. Passivation is to make the polymeric surface inert to platelet-binding proteins. Recently, the immobilization of a heparin-albumin conjugate was also investigated to increase the thromboresistance of biomedical polymers [Bos *et al*, 1999]. However, some problems still exist with such methods. The immobilized active proteins are susceptible to conformational changes and enzymatic deterioration *in vivo* and are often suitable for

3

only short-term applications. To date, none of these methods generate a complete non-thrombogenic surface [Muntean, 1999].

Nitric oxide (NO), a small messenger molecule, serves to inhibit platelet adhesion, aggregation, and activation as well as relax smooth muscles and modulate neurotransmission [Moncada *et al.*, 1991, Radomsk and Moncada, 1993], as discussed in detail in Chapter 2. Vascular endothelial cells synthesize and release NO and prostacyclin to make vessel walls completely compatible with platelets [Radomski *et al.*, 1987a; Moncada *et al.*, 1990; MacAllister and Vallance, 1996]. To mimic NO release from the inner surface of the blood vessel, significant research has been devoted to the incorporation of diazeniumdiolate NO donors into polymer surfaces to reduce platelet adhesion, aggregation, and thrombus formation on blood-contacting surfaces [*Mowery et al.*, 2000].

Hanson *et al.* (1995) reported that vascular grafts coated with diazeniumdiolates were less susceptible to platelet adhesion whereas control grafts were sealed with thrombus after 1 hr within a circulatory system of a baboon. Another study conducted in baboon's circulatory showed that diazeniumdiolate donors can be incorporated into polymers to dramatically improve the polymer's biocompatibility [Smith *et al.*, 1996]. Annich *et al.* (2000) showed that NO donors entrapped in rabbit's venous extracorporeal circuits can inhibit platelet adhesion and aggregation on the surface of the circuit. In addition, localized NO release from NO donors incorporated in chemical sensors exhibited significantly reduced platelet adhesion / activation and improved the analytical performance *in vitro* [Espadas-Torre *et al.*, 1997] and *in vivo* within the arteries of dogs as illustrated in Figure 1.1 [Schoenfisch *et al.*, 2000]. An ultrafast NO donor,

PROLI/NO, developed by Saavedra *et al.* (1996), inhibited thrombus formation and induced selective dilation of the vasculature. Other NO-releasing polymers, described by Mowery *et al.* (2000), were not favorable for platelet adhesion when exposed to sheep's platelet rich plasma.
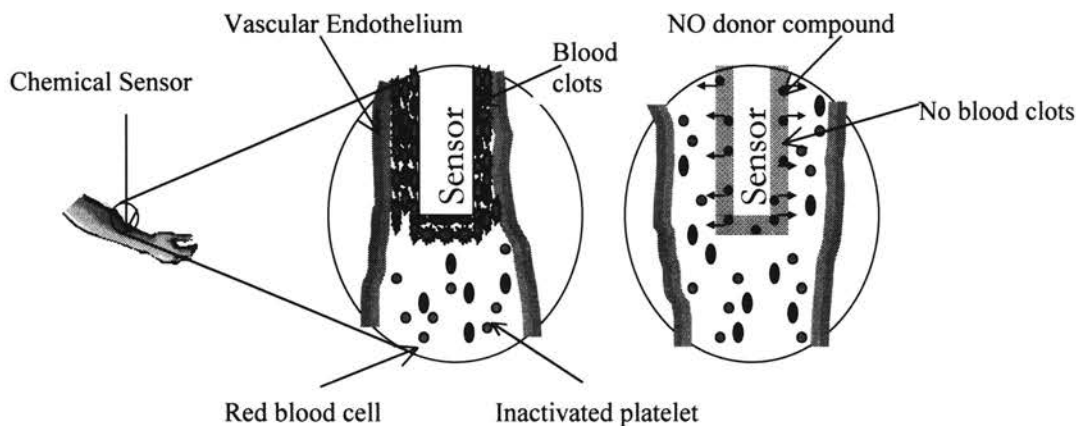
Figure 1.1 Schematic of (a) typical problems associated with current blood sensors and (b) how the problems are solved when the sensor is coated with NO donors. Figure adapted from Schoenfisch *et al.*, 2000.

All the above investigations demonstrate that localized NO release through incorporating NO donors into polymer surfaces may be an effective strategy for solving the haemocompatibility problems associated with blood-contacting medical devices. However, some limitations of NO-releasing polymer must still be resolved, which, if not resolved, may limit the applications of this technology. The potential limitations include:

(a) Non-constant release rate. To date, all the diazeniumdiolate NO donors display first-order decomposition of NO when exposed to aqueous solution. The initial high release rate may lead to cytotoxic and mutagenic effects [Hibbs *et al.*, 1987; Tamir *et al.*, 1996; Keshive *et al.*, 1996; Fehsel *et al.*,

1996] whereas a low release rate may not be enough to inhibit platelet adhesion and aggregation [Diodati *et al.,* 1993].

(b) Limited life span. Since only a limited amount of NO moiety can be incorporated into the surface of a polymer, the release of NO donors will eventually stop. The life of current NO donors entrapped in polymers may vary from several hours to several weeks [Mowery *et al.* 2000]. Thus, NO releasing polymers can only be applied for short-term applications.

(c) Toxic concerns from donor residues. The dissociation of diazeniumdiolates during the release of NO can be accompanied with the release amines depending upon the method of incorporation. Thus, potential carcinogens may form in the presence of NO (i.e., nitrosamines) [Loeppky, 1994; Mowery *et al.,* 2000].

(d) Change of polymer properties. The change of mechanical properties following NO-donor incorporation is also a potential complication of NO donor-modified polymers.

In this thesis, a novel method for improving the haemocompatibility of biomaterials through exploiting endogenous NO for localized NO release is advanced. Briefly, NO bound to serum albumin (S-nitroso-albumin) in human plasma can be transferred to L-cysteine immobilized onto the surface of polymeric biomaterials through transnitrosation. S-nitroso-L-cysteine formed following transnitrosation is very unstable and releases NO under the attack of naturally present metal ion in blood (e. g., copper). The NO release from S-nitroso-L-cysteine (CySNO) will then inhibit platelet adhesion. The rationale for developing this novel idea is elaborated in Chapter 2. This method may

eventually eliminate the above disadvantages of NO-releasing polymers since occurring NO in human blood is utilized. The experimental evidence showed in Chapter 5 fully supports the proposed mechanism and demonstrates that it is feasible to improve the haemocompatibility of existing blood-contacting polymers via endogenous NO utilization. This technology may eventually be applied on the medical devices mentioned in Table 1.1.

CHAPTER 2

LITERATURE REVIEW

Following injury to a blood vessel, platelets are utilized to stop bleeding. The discrete series of steps to stop bleeding include platelet adhesion to the damaged blood vessel (e.g., collagen), platelet activation due to agonists (e.g, thrombin), platelet aggregation via fibrinogen, and finally thrombus formation. However, this same process may generate adverse consequences when foreign polymeric surfaces are placed in contact with blood. The potential complications for the blood-contacting medical devices include reducing the performances of the medical devices and causing harm to or even death of patients as described in Chapter 1. In this chapter, sufficient background information is presented to demonstrate how the haemocompatibility of blood-contacting materials can be improved using endogenous NO.

Briefly, the mechanisms of the coagulation and the thrombogenesis due to platelet interactions with artificial surface are reviewed. Then naturally occurring inhibitory mechanisms of platelet activation and aggregation are described, in which nitric oxide (NO) is a key component. Subsequently, the chemistry and physiology of S-nitrosothiols (the adduct of NO and thiol) are discussed in detail since the properties of endogenous S-nitrosothiols (S-nitroso-proteins) and S-nitroso-L-cysteine are critical to the proposed mechanisms of endogenous NO utilization. Finally, the rationale for the idea of using endogenous NO to improve the haemocompatibility of biomaterials will be summarized.

2.1 Platelet interactions with artificial surface

2.1.1 Platelet structure

Platelets, previously described as "sponges" [Adelson *et al*., 1961], are anucleate, disk-shaped cells (Figure 2.1) having a diameter of 3-4 μm, a thickness ~1 μm, and an average volume of ~10 μm^3 [Frojmovic *et al*., 1976]. Platelets are produced by megakaryocytes in the bone marrow and have a life span of 8 to 12 days in humans [Tessier et al., 1974]. Platelets circulate at an average concentration of about 250,000 cells/μl, ranging from 140,000 to 440,000 cells/μl and account for approximately 0.3% of the total blood volume. Platelet structure, as shown in Figure 2.2, is essential to maintain the normal platelet functions. The important constituents/organelles that play essential roles in platelet adhesion and aggregation are discussed as follows.

Plasma membrane. The platelet membrane is a typical trilaminar membrane with glycoproteins and glycolipids embedded in a phospholipid bilayer [White and Clawson, 1980^a]. Many of the glycoproteins, acting as receptors, mediate a wide number of adhesive cellular interactions. The two principal receptors are glycoprotein (GP) IIb/IIIa and GP Ib-IX. A Ca^{2+}-dependent conformational change in GP IIb/IIIa after platelet activation can lead to strong binding to fibrinogen [Sims et al., 1991] and von Willebrand factor (vWF) [Savage *et al*., 1996], which is responsible for platelet aggregation due to fibrinogen cross-linking. Each inactivated platelet contain 40,000 to 80,000 copies of GP IIb/IIIa on the membrane surface [Phillips *et al*., 1988] and ~30,000 copies of GP IIb/IIIa

Figure 2.1. Scanning electron micrograph of inactivated human platelets. Most are discoid (d) in shape. The surface indentations, indicated by arrows, are the surface-connected canalicular system to the external milieu (From Stenberg *et al.*, 1984).
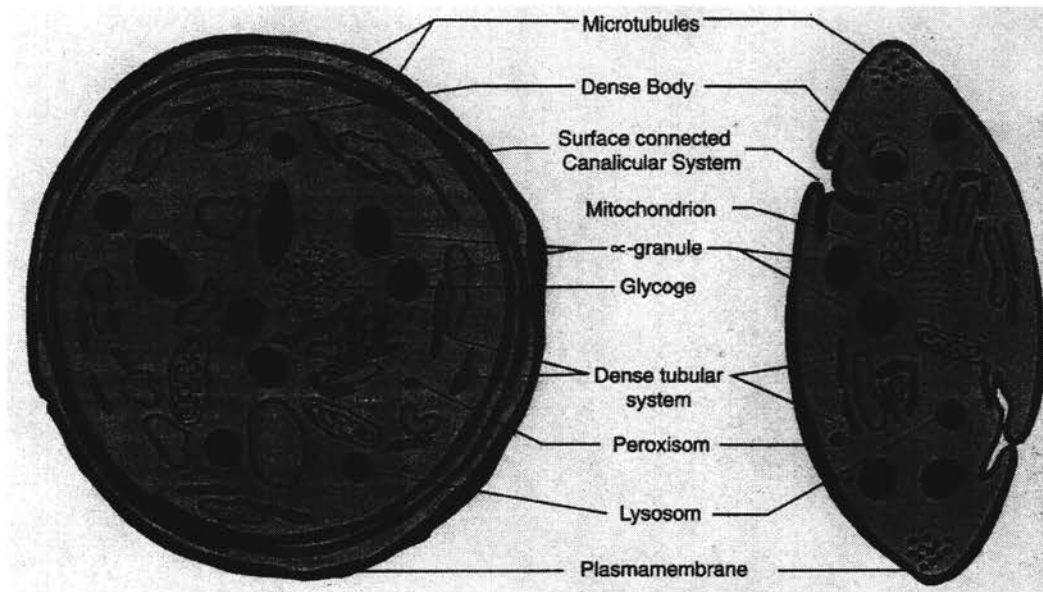
Figure 2.2. Diagram of a human platelet displaying components visible by electron microscopy and cytochemistry. Membranous componets include plasma membrane, surface-connected canalicular system, and dense tubular system. Four types of storage organelles are α-granules, dense bodies, lysosomes, and microperoxisomes. (From Bentfel-Barker *et al.*, 1982).

on α-granule and canalicular system membranes, which can move to plasma membrane after activation [Cramer *et al.*, 1990]. GP Ib-IX is a binding site for collagen, vWF, and thrombin [Ruggeri, 1991] and is a primary receptor for adhesion at injury sites and then trigger platelet activation. Other membrane glycoproteins such as GP Ia-IIa and GP Ic-IIa mediate platelet binding to collagen, fibronectin, and vitronectin.

Membrane phospholipids also play a role in platelet activation and clot formation. Arachidonic acid can be liberated from the membrane phospholipids by the direct action of phospholipase A_2. The intracellular arachindonic acid is metabolized into prostaglandins PGG_2, PGH_2, PGD_2, and PGI_2 via cycloxygenase [Adams, 1985[a]]. PGG_2 and PGH_2 are the precursors of thromboxane A_2 (TxA_2) that is considered as the stimulant of platelet aggregation. PGD_2 and PGI_2, which are prostacylin, can inhibit the platelet adhesion and aggregation by raising intracellular cyclic adenosine monophosphate (cAMP) level.

Surface-connected canalicular system. The surface-connected canalicular system weaves throughout the cell cytoplasm in a tortuous way. It was showed that this system is in direct continuity with the plasma membrane and the external milieu [White and Clawson, 1980[b]]. The functions of this system are to provide a route of entry and exit for molecules, an internal reservoir of membrane to facilitate platelet spreading and pseudopodia formation after adhesion, and a storage reservoir for membrane glycoproteins that increase on the platelet surface after activation [Cramer *et al.*, 1990; Suzuki *et al.*, 1992].

Cytoskeleton. The platelet cytoskeleton consists of three major structural components: an actin microfilament network present throughout the cytoplasm [Boyles *et*

al., 1985], a microtubule coil localized at the platelet periphery [White and Sauk, 1984], and a membrane skeleton underlying the inner surface of the plasma membrane [Fox et al., 1988]. Actin microfilaments containing substantial muscle proteins (e.g., actin and myosin) are responsible for developing filopodia (A long spike protruding from the growing tip on cell) via polymerization and phosphorylation during activation [Fox and Phillips, 1982; Hartwig, 1992]. Microtubules re-assembly during platelet activation results in the alteration of the platelet shape from discoid to round. Membrane skeleton may take part in platelet spreading after adhesion and mediate signal transduction [Fox *et al.,* 1993].

α-granules. α-granules are the predominant granule type in the platelet with a diameter varying from 300 to 500 nm. Several important proteins involving platelet activation and aggregation are present in the granular compartment and on the membrane of α-granules, including platelet factor 4 [Harrison *et al.*, 1990], vWF, fibronectin, fibrinogen [Wencel-Drake *et al*, 1985], coagulation factor V [Hayward *et al.*, 1995], and GP IIb/IIIa [Cramer *et al.*, 1990]. Platelet factor 4 enhances the platelet aggregation by neutralizing the anticoagulant activity of heparin. Factor V is one important component of the prothrombinase complex that converts prothrombin into thrombin, which is a potent agonist for platelet activation.

Dense granules. Dense granules are approximately 200-300 nm in diameter and are the organelle with the highest density in platelets (1.2 g/ml). The principal constituents of dense granules are a nonmetabolic reservoir of adenosine diphosphate (ADP), adenosine triphosphate (ATP), Ca^{2+}, and serotonin. The release of ADP after stimulation can trigger the activation of the surrounding platelets. Ca^{2+} is considered as

the most important single intracellular mediator of platelet functions [Authi, 1993] since many enzymatic processes during platelet activation are calcium-dependent as discussed in Section 2.1.2.

Lysosomal granules. Lysosomal granules are small vesicles with a diameter of 175-200 nm. These granules contain a large variety of enzymes, including β-glycerophosphatases and acid hydrolases. Lysosomal constituents are released more slowly and incompletely than α- and dense granules after stimulation, suggesting they play a greater role in anticoagulation than in hemostatic response [White, 1993].

2.1.2 Platelet Adhesion and Aggregation

Platelets adhere to an injured blood vessel wall to prevent blood loss via a series of steps involving platelet adhesion to the wounded area and platelet activation. Platelet activation is the generation of intracellular chemical signals that are initiated by platelet adhesion and soluble agonists that stimulate the platelet through specific receptors. The platelet activation causes rapid morphologic changes such as the formation of spiny pseudopods, granule secretion, and the expression of fibrinogen receptors that results in platelet-platelet aggregation.

Platelet adhesion. At sites of vessel injury, the platelet adhesion process involves the interaction of membrane receptors with a rich matrix of subendothelial proteins, including collagen, von Willebrand factor, fibronectin, and fibrinogen. The specific interactions of these proteins with platelets *in vivo* are discussed as follows.

Collagens are the major components of the blood vessel wall and the important contributors to the platelet adhesion and hemostasis. The vessel wall contains several

different types of collagens which have corresponding different binding abilities to the platelet membrane protein GPIb-IX or GP Ia-IIa. In addition, flow conditions also affect the binding of platelet to subendothelial collagens [Saelman *et al.*, 1994].

von Willebrand factor (vWF) is a large adhesive protein that is located in the vasculature including the subendothelium and plasma. Upon blood vessel injury, vWF is exposed and mediates platelet adhesion via binding to GPIb-IX receptors on the platelet membrane [Berndt *et al.*, 1995]. vWF in plasma does not bind to GPIb-IX because vWF is at the inactive form in plasma whereas it is in the active conformation in endothelium [Berndt *et al.*, 1995].

Fibronectin is a two-subunit subendothelial extracellular matrix protein that is also present in platelet α-granules and plasma. Platelets adhere to fibronectin via multiple mechanisms. These mechanisms involve platelet adhesion via either GPIIB/IIIa or GPIc-IIa binding to the RGD amino acid sequence located in the domain of fibronectin [Bowditch *et al.*, 1994].

Fibrinogen is mainly responsible for platelet aggregation as well as its important role in platelet adhesion. The fibrinogen concentration in human plasma is as high as ~2.5mg/ml. The fibrinogen molecule has molecular mass of 340 kg/mole and is a large trinodular disulfide-bonded glycoprotein composed of two symmetric half-molecules (Figure 2.3). Each half-molecule contains three distinct polypeptide chains called the Aα, Bβ, and γ chains. The entire molecule is 45 nm long and 9 nm in diameter [Doolittle, 1983]. The amino-terminal portions of these chains are disulfide-linked, forming the central E domain. The C-terminal portions of these chains are present in the

D domains [Weisel *et al.*, 1985]. The major platelet binding site is located at the carboxyl-terminus of the fibrinogen γ chain.
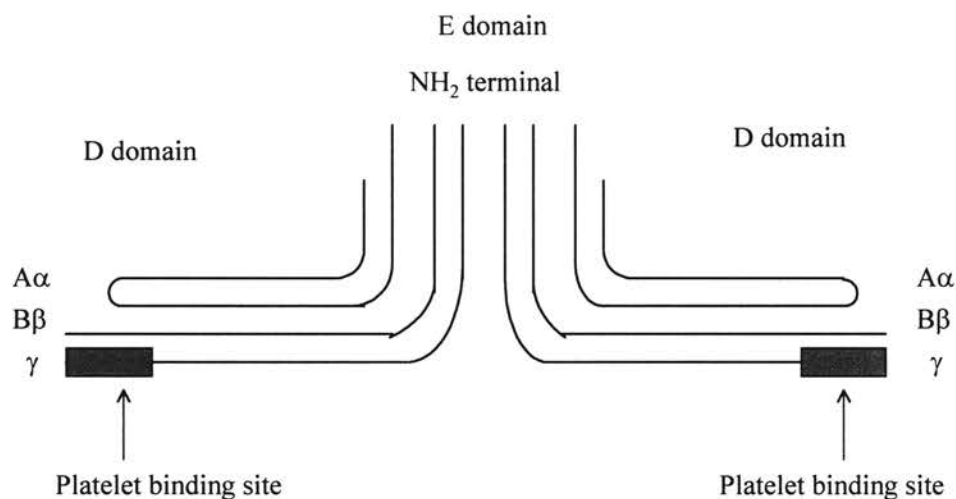
Figure 2.3. Structure of fibrinogen. Fibrinogen is composed of three domains: two D domains and one E domain. The platelet binding sites are located at the C-terminus of the γ chain. Aα is a 610-amino acid polypeptide that has a α-helix domain. Bβ is a 460-amino acid polypeptide that has a coiled-coil domain. γ is a 411-amino acid polypeptide and its C terminal section is a globular subdomain. Figure modified from Mosesson, 1990.

Platelet adhesion to the surface of blood-contacting polymers may also be mediated through platelet GP IIb/IIIa and GP Ib-IX. Normally inactivated GPIIb/IIIa receptors do not bind to ligands such as fibrinogen, vWF, and fibronectin. However, some of these protein usually undergo conformational changes as a result of the adsorption process and then are susceptible to react with GPIIb/IIIa [Ratner *et al.*, 1995]. Then the surrounding platelets near surface can be activated by exposure to agonists released from the adherent cells. The expression of competent GPIIb/IIIa receptors will

support tight binding and platelet spreading through multiple focal contacts with fibrinogen and other surface-adsorbed adhesive proteins.

Platelet aggregation. Following platelet adhesion, a complex series of reactions is initiated, including (i) the release of dense granule ADP, (ii) the formation of thrombin on the surface of activated platelets, and (iii) the activation of platelet signal transduction of generating thromboxane A_2(TxA_2). These released agonists cause platelets to change shape such that they form long pseudopodia and express/activate the platelet adhesion receptor GP IIb/IIIa. The activated GP IIb/IIIa can bind fibrinogen or vWF and link adjacent platelets together, which result in platelet aggregation.

The release of constituents from platelets is initiated in response to agonists, such as thrombin, collagen, and ADP, acting on specific membrane receptors. These agonists interact with their own receptors evoking an intracellular signal. This signal is carried by messenger molecules to the granules, fusing them with the membrane of the surface-connected canalicular system through which stored molecules are released. The extent of secretion depends on the strength of the agonist. Weak agonists (e.g., ADP) require both cyclooxygenase activity and primary aggregation to induce secretion. Strong agonists (e.g., thrombin and collagen) at high concentrations induce platelet aggregation and secretion that is independent of cyclooxygenase activity [Siess *et al.*, 1983], whereas at low concentrations they induce aggregation and secretion that is entirely dependent on cyclooxygenase activity and released ADP.

The interaction of the platelet receptors with the specific agonists including collagen, thrombin, TxA_2, platelet-activating factor (PAF), and ADP causes a cascade of inside-out signaling events that lead to the activation of fibrinogen receptor GPIIb/IIIa

16

(Fig. 2.4), which is the important consequence of platelet activation. Some signaling pathways involved in platelet activation are reasonably well known, whereas others are not. Most of the agonists activate platelets by occupying transmembrane-spanning, G-protein-coupled receptors. Figure 2.5 schematically illustrates three stimulatory pathways in human platelets.

The first pathway involves archidonic acid, which is generated through phospholipid hydrolysis by phospholipase A_2 under the cooperation of Ca^{2+} and then transformed by cyclooxygenase into TxA_2. The formed TxA_2 diffuses out of the cell and causes further platelet activation (self-reinforcing). In the presence of Ca^{2+}, the phospholipase C activation due to the interaction of platelet receptors with agonists can hydrolyze phosphatidylinositol 4,5-bisphosphate (PIP_2), generating diacylglycerol (DAG) and inositol 1,4,5-triphosphate (IP_3). In the presence of Ca^{2+}, DAG activates protein kinase C which subsequently phosphorylates low molecular weight G protein to cause secretion and activation of GPIIb/IIIb through unknown mechanisms. This process is defined as second signaling pathway. The last pathway involves the intracellular Ca^{2+} release from the dense tubular system due to the IP_3 interaction with specific receptors [Knezevic et al., 1992]. The increased intracellular Ca^{2+} concentration can activate myosin light chain kinase, which is associated with the platelet secretion [Hawiger, 1989]. Also the activation of GPIIb/IIIb only occurs at the elevated intracellular Ca^{2+} concentration.

As an intracellular messenger, Ca^{2+} is involved in several key steps in all the three signaling pathways as indicated in Figure 2.5. Therefore, molecules that can reduce or
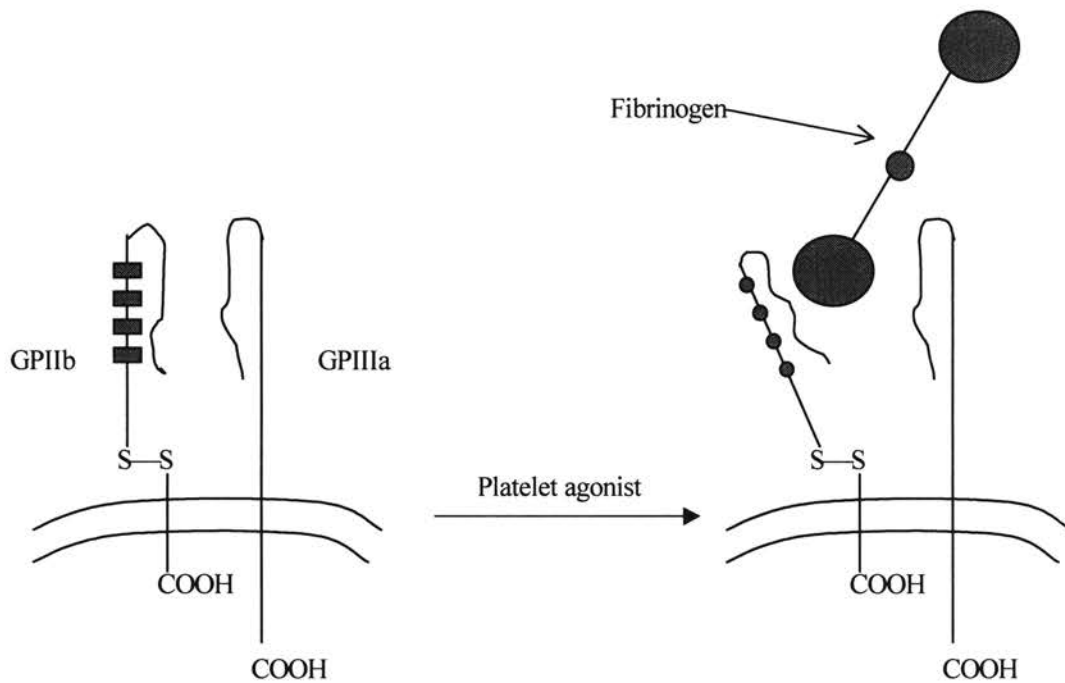
Figure 2.4. Structure and activation of the platelet fibrinogen receptor integrin GPIIb/IIIa. This integrin is composed of two subunits. The bulk of the integrin is extracellular with short cytoplasmic domains that involve regulating the conformation and function of the integrin. The GPIIb/IIIa exists in a resting conformation on unstimulated platelets. Following stimulation by agonists, the integrin is activated so that the amino terminal ends of the two subunits form a binding pocked for fibrinogen. Bound fibrinogen crosslinks platelet together in an aggregate. Figure adapted from Sims *et al.*, 1991.
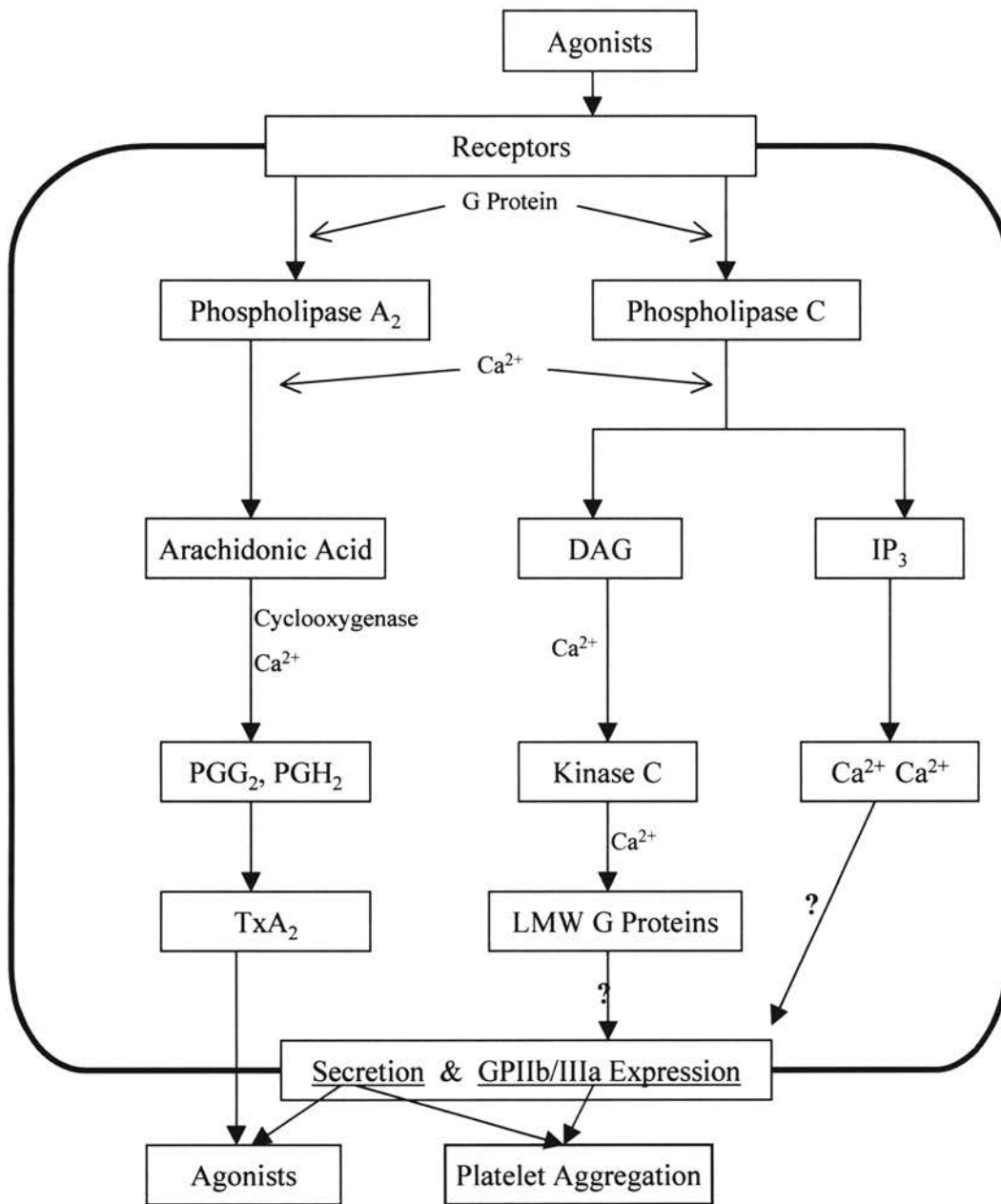
Figure 2.5. A simplified scheme of signal transduction pathways in platelet activation. The interactions of receptors with agonists result in the generation of TxA_2, fibrinogen binding receptor (GPIIb/IIIa) expression, and platelet secretion. Secreted agonists and generated TxA_2 cause further activation. GPII/IIIa expression can be bound by fibrinogen and lead to aggregation under the help of the secreted Ca^{2+}. DAG: diacylglycerol. IP3: inositol 1,4,5-triphosphate. PGG_2: prostaglandins G_2. PGH_2: prostaglandins H_2. TxA_2: Thromboxane A_2. ? means the mechanism is unknown. Figure modified from Hawiger, 1989.

remove Ca^{2+} in the platelet can inhibit platelet adhesion and activation. Both prostacyclin and nitric oxide released from endothelial cells generate antiplatelet effects, at least partially, through this mechanism (reducing intracellular Ca^{2+} concentration), which is discussed later. In Chapter 5, Acid-citric acid-dextrose (ACD) is employed to prevent platelet activation and activation during the preparation of platelet suspension because ACD can chelate Ca^{2+} [Mustard et al., 1989]. Other chelators such as EDTA have been shown to have anicoagulant effects, which is also through this mechanism.

2.1.3 Coagulation (Thrombus Formation)

Thrombus formation is the normal, physiologically important outcome of primary hemostasis. As discussed in the last section, platelets adhere to the injury site, secret factors that further activate and recruit local platelets, and aggregate to form a platelet plug. However, this platelet plug is not strong enough to block bleeding and stand blood flow stress unless it is fortified with the meshwork of a fibrin gel, which is accomplished by a cascade of platelet coagulant activities.

Fibrin is formed upon cleavage of soluble fibrinogen by thrombin to release fibrinopeptides A and B. These peptides are cleaved from the amino-terminal end of the Aα chain and the Bβ chain, respectively [Blomback, 1994]. Fibrin spontaneously polymerizes to form an insoluble gel to fix the platelet aggregate, which is called a thrombus. Platelets bind to soluble fibrinogen and insoluble fibrin through their GPIIb/IIIa receptors to nucleate and immobilize the fibrin clot.

Platelets enhance fibrin formation by forming a catalytic surface for the assembly of procoagulant enzymes (factor IXa factor VIIIa) that convert prothrombin to active thrombin. Platelets become catalytic for these procoagulant enzymes by exposing anionic phospholipids, most important phosphatidylserine (PS), on the platelet surface following platelet activation. How anionic lipid exposure actually occurs is elusive, which may involve the inhibition of an aminophospholipid translocase that normally serves to maintain phospholipids distributed asymmetricaly in the platelet membrane [Kirchhofer et al., 1995]. Upon exposure of PS on the platelet surface, a complex consisting of PS, factor IXa and factorVIIIa is assembled, enhancing the activation of factor X by factors IXa and VIIIa [Mann et al., 1990]. The prothrombinase complex of factor Xa and Va on the platelet membrane that converts prothrombin into thrombin so that thrombin can convert fibrinogen to fibrin to stabilize the hemostatic plug. Factors IXa, X, and prothrombin bind to platelets via Ca^{2+} bridge formation between these factors and the negatively charges phospholipid on the platelet membrane [Bevers et al., 1993].

When the thrombus is formed on the foreign surface such as polymer and glass, the platelet cohesion is stronger than platelet adhesion so that embolization (thrombus detachment) may be formed under the forces exerted by the blood [Adams, 1985[b]]. Embolization usually occurs when a thrombus reaches a characteristic size under a specific flow condition. The cyclic growth of thrombi and subsequent emoblization is a major concern in the applications of blood-contacting biomaterials. As discussed in Chapter 1, emboli may cause life-threatening stroke for patient and interfere with the performance of medical devices.

From the above description, a full picture about the events in the formation of a thrombus on an injured blood vessel or biomaterials is presented in Figure 2.6. If the thrombogenic surface is an injured blood vessel, the interaction between the subendothelial surface and platelet is usually strong enough to stand the flow shear stress. Therefore, embolization normally does not occur on the injured blood vessel. However, the cyclic thrombus formation and embolization may occur on the surface of foreign biomaterials as discussed above.

Thromogenic Surface

Cyclic

Platelet Adhesion (<1 Sec)

Platelet Spreading

α-Granule Release   Dense-Granule Release   Arachindonic acid

Fibrinogen; vWF; PF4 Ca^{2+}; ADP   TxA2

Platelet Aggregation

Prothrombin ⟶ Thrombin ⟶

Fibrinogen

Fibrin

Coagulation (Thrombus) ———— Embolization ————

Blood Clot
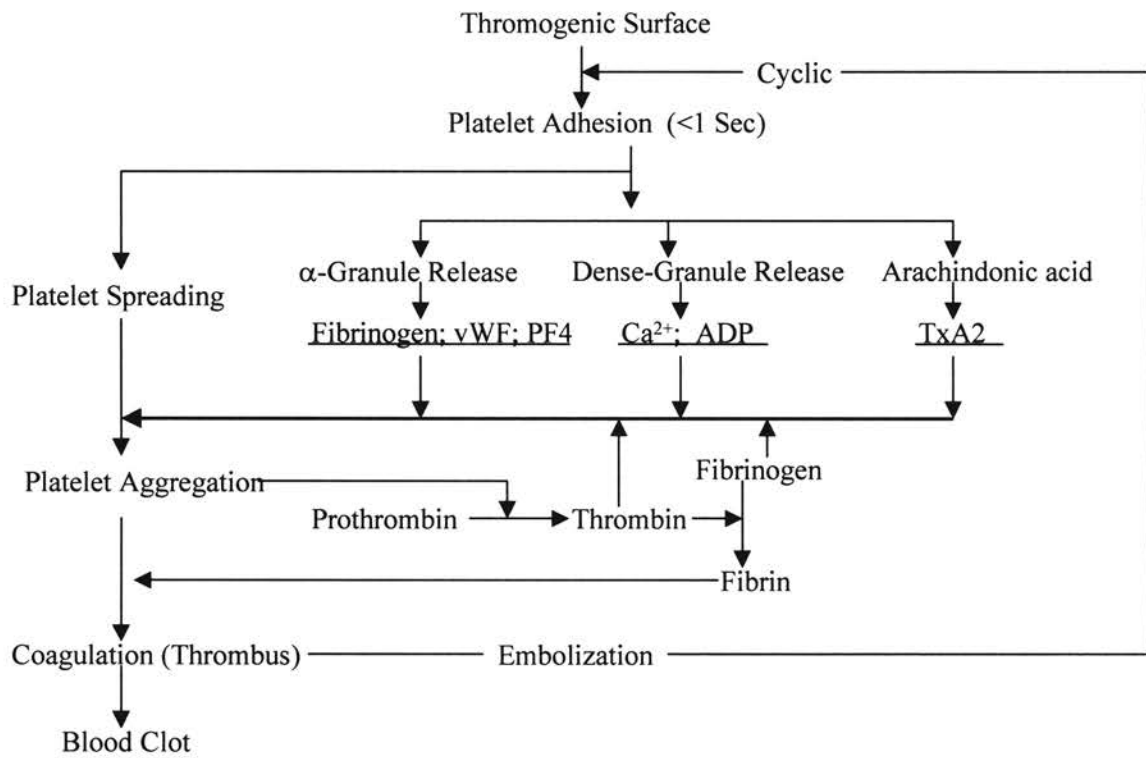
Figure 2.6. A paradigm of integrated hemostatic reaction between platelets and a thrombogenic surface (injured blood vessel or foreign biomaterials). Figure modified from Adams, 1985[b]

2.2 Natural inhibitory mechanisms of platelet activation and aggregation

The formation of a platelet plug at the site of vascular injury is highly localized and transient. The platelet plug normally does not grow uncontrollably and block blood flow. In contrast, the formed clot will be removed (fibrinolyzed) when the injury is healed. Furthermore, an uninjured blood vessel wall is totally compatible with platelets (nonthrombogenic). Therefore, a variety of mechanisms must exist *in vivo* to prevent platelet adhesion to uninjured endothelium and to limit platelet aggregation and thrombus growth on an injured vascular wall. The main mechanisms include the anticoagulant pathways, the fibrinolytic system, and the production of prostacyclin and nitric oxide (NO)

2.2.1 The anticoagulant pathways

The first anticoagulant pathway involves thrombomodulin (TM), a transmembrane protein prevalent on the surface of endothelial cells. TM functions as a high-affinity receptor for thrombin, which it binds with a 1:1 stoichiometry. Thrombin bound to TM alters its functional properties including the decreased ability to convert fibrinogen into fibrin, activate factor V (procoagulant protein), and stimulate platelets [Esmon, 1982, Esmon, 1983]. The binding of thrombin to TM also accelerates the inhibition of the thrombin by antithrombin III [Preissner *et al.*, 1986].

Another important role of TM in anticoagluation is that the TM-thrombin complex can initiate the protein C anticoagulant pathway. Protein C is a glycoprotein present in human plasma, which is converted to activated protein C (APC) by the TM-thrombin complex in a Ca^{2+}-dependent manner [Owen and Esmon, 1981]. APC is a

serine proteinase that inactivates factor VIIIa and Va via limited proteolysis, thus inhibiting the generation of two key enzymes, factor Xa and thrombin [Suzuki *et al.*, 1983; Eaton *et al.*, 1986]. This function of APC is enhanced by Ca^{2+} and a plasma glycoprotein S [Hanson *et al.,* 1993].

Naturally occurring antithrombin III (ATIII) is also potent inhibitor of thrombin and other coagulation enzymes (e.g., IXa and Xa). ATIII is synthesized in liver and present in plasma at a concentration of 125 µg/ml. Heparin and heparan sulfate (a heparin-like molecule) can augment the rate of ATIII inhibition of these enzymes by several thousand-fold. Thus it is believed that the inhibition of coagluants by ATIII is carried out on the membrane of endothelial cells since heparan sulfate is present on the surface of endothelial cells [de Agostini *et al.*, 1990].

2.2.2 The fibrinolytic system

The fibrinolytic system removes the fibrin clot (degrading fibrin) once it has achieved its hemostatic function. Fibrinolysis is carried out by the production of plasmin from plasminogen. The function of the generated plasmin is to degrade the fibrin clot and extracellular matrix molecules [Gurewich, 2000].

Plasminogen is synthesized in the liver and circulates in plasma at a concentration of ~200 µg/ml, which can be activated by tissue-type plasminogen activator (t-PA) as well as urokinase-type plasminogen activator (u-PA). t-PA is predominantly an endothelial cell enzyme and can be released from endothelium by stimuli such as thrombin and shear stress [Diamond *et al,* 1989]. In normal human plasma, t-PA is present at an extremely low concentration (0.1 nM), in which more than 95% of t-PA is

inactive since it forms a complex with its natural inhibitor [Redlitz and Plow, 1995]. Therefore, the released t-PA from endothelial cells is mainly responsible for conversion of plasminogen to plasmin. The catalytic efficiency of t-PA is enhanced several hundredfold when t-PA and plasminogen bind on the fibrin surface, which is vital to the physiological function of t-PA [Loscalzo, 1988]. Thus, the activator of plasminogen by t-PA is supposed to be carried out on the fibrin surface since plasminogen also has a binding site for fibrin.

u-PA was first identified in the urine [Husain *et al.*, 1983] and subsequently detected in endothelial cells and plasma [van Hinsbergh, 1988]. u-PA is also a serine proteinase and synthesized as a single-chain molecule called single-chain u-PA (scu-PA). scu-PA has a very low level of proteolytic activity, whereas two-chain u-PA (tcu-PA) converted from scu-PA by plasmin has a high efficient enzyme. It has been proposed that scu-PA is a true zymogen with no activity toward plasminogen. Cleavage of plasminogen to plasmin would occur only when scu-PA is converted to tcu-PA [Gurewich *et al.*, 1987]. The mechanism by which scu-PA is converted into tcu-PA remains to be defined. It has been protulated that a small amount of t-PA initially generates plasmin which then rapidly converts scu-PA into tcu-PA [Gurewich *et al.*, 1987]. This process results in amplification of fibrinolytic activity.

Besides secreting plasminogen activators, endothelial cells also have the binding receptors for plasminogen and plasminogen activators including t-PA and u-PA [Hajjar and Hamel, 1990]. Receptors for both plasminogen and its activators function to accelerate plasminogen conversion to plasmin [Hajjar, 1991; Plow *et al.*, 1995].

A variety of natural inhibitors to fibrinolysis exist in plasma and blood cells. α2-antiplasmin, directly inhibiting plasmin by binding the active site, and PAI, inhibiting the activation of plasminogen by forming inactive complex with t-PA, play a dominant role in regulating fibrinolysis. Figure 2.7 summaries how the fibrinolytic activity is regulated *in vivo.*
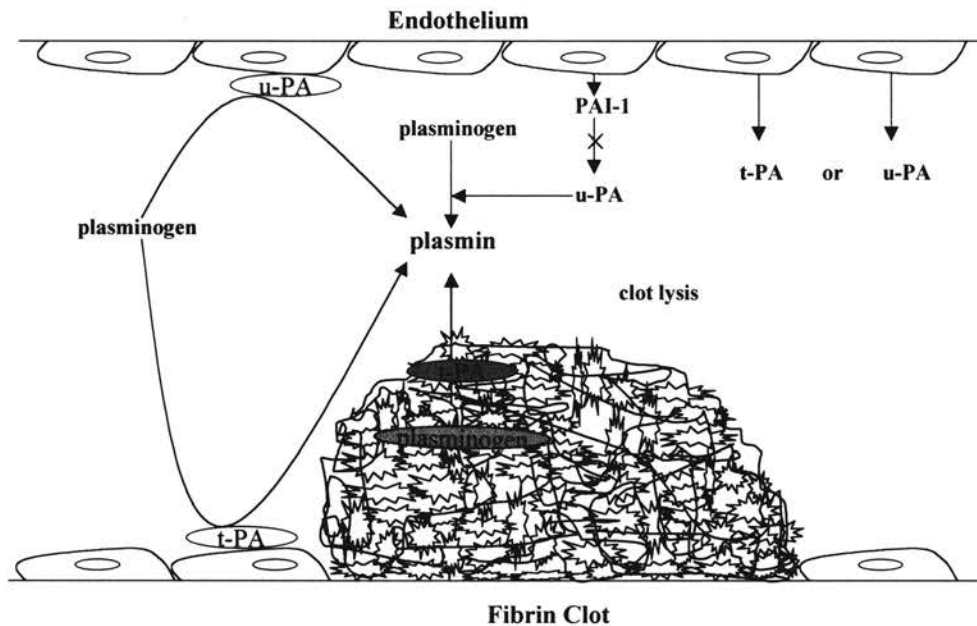
Figure 2.7. Regulation of plasminogen activation *in vivo*. Activation of plasminogen occurs at three different interfaces: (i) plasma interaction; (ii) endothelial cell-mediated interactions; (iii) clot-bound events. In plasma, activation of plasminogen occurs through two-chain u-PA. The circulating inhibitor of u-PA (PAI-1) effectively limits this activation pathway. Endothelial cells have receptors for u-PA, t-PA, and plasminogen and the conversion of plasminogen into plasmin is carried out on the cell surface, which is more efficient than the process in the plasma. Finally, conversion of plasminogen to plasmin also occurs in the clot and is enhanced by fibrin. Plasminogen and t-PA specifically bind to a fibrin clot formed at the site of vascular injury. PAI-1 released from activated platelets in the clot can also lower the conversion of plasminogen to plasmin (not shown in the figure). Figure adapted from Plow *et al.*, 1995.

2.2.3 Prostacyclin and nitric oxide (NO)

The above two mechanisms (the anticoagulant pathways and the fibrinolytic system) are designed to avoid massive thrombus formation once coagulation is initiated. Prostacyclin and NO produced and released from endothelial cells are responsible for inhibiting the initial stage of hemostasis: platelet adhesion and platelet aggregation. The following describes how these two potent factors regulate platelet-vessel wall interactions.

Prostacyclin (PGI$_2$). Prostacyclin is the metabolic product of arachidonic acid, where the endothelial cells are the principal source. Prostacyclin is relatively unstable, with a half-life of 2-3 mins. Release of prostacyclin can be stimulated by mechanical or chemical stimuli. Prostacylin is the most potent endogenous inhibitor of platelet aggregation yet discovered [Moncada *et al.*, 1990]. Usually it is employed to inhibit platelet activation and aggregation during the preparation of platelet suspensions for the purpose of research or clinics [Shahbazi *et al.*, 1994; Radomski *et al.*, 1996]. The duration of the effects of prostacyclin *in vivo* is about 30 min after administration [Moncada, 1982].

Prostacyclin inhibits platelet aggregation in a cyclic adenosine monophosphate (cAMP)-dependent manner. It interacts with specific G protein-coupled receptors on the platelet surface, resulting in the activation of adenylate cyclase, which induces the formation of cAMP. The extent of cAMP production is balanced by phosphodiesterase activity, which breaks down cAMP. The elevated cAMP activates cAMP-dependent kinases (also called protein kinase A), which phosphorylate specific proteins, presumably inhibiting platelet reactivity. The exact targets of cAMP-dependent kinases that result in

an inhibition of platelet reactivity are not entirely clear, although several possibilities exist and inhibition may occur at more than one point in more than one pathway. For example, it has been demonstrated that elevated cAMP inhibits the IP3 receptor in platelets by the phosphorylation of this receptor, resulting in a decrease in intracellular Ca^{2+} levels [Cavallini *et al.,* 1996]. It was also reported recently that elevated cAMP also inhibits the thrombin-induced phospholipase C and A_2 activations as well as prevents the thrombin-induced increase in cytosolic Ca^{2+} level [Nishimura *et al.,* 1995], although the mechanism is not clear.

Prostacyclin reduces platelet adhesion to exposed vascular subendothelium at a concentration two hundred times as much as the concentration required to prevent platelet aggregation [Higgs *et al.,* 1978]. This suggests that prostacyclin released by endothelial cells plays a minor role in platelet adhesion, although it is effective in preventing or limiting thrombus formation by inhibiting platelet aggregation [Moncada, 1990].

Nitric oxide (NO). Furchgott and Zawadzki (1980) demonstrated that blood vessels induced by acetylcholine were dependent on the presence of the endothelium and this effect was mediated by a factor which they later named endothelium-derived relaxing factor (EDRF). In 1987, Palmer *et al.* provided evidence that cultured endothelial cells synthesized NO, that NO and EDRF were pharmacologically identical, and that NO accounted for the biologic activity of EDRF. To date, an overwhelming amount of evidence had accumulated that NO is the true identity of EDRF [Ignarro *et al.,* 1999].

In healthy blood vessels, NO/EDRF is mainly produced in endothelial cells by the constitutive NO synthase enzyme. Under certain pathophysiolgical conditions (e.g., injured blood vessel), various other types of vascular cells including smooth muscle cells,

macrophages, and fibroblasts are induced to produce NO via the inducible NO synthase [Busse *et al.,* 1995]. NO generated by this pathway is considered to account, at least in part, for the cytotoxic effects of macrophages and thus play a crucial role in host defense.

NO synthases oxidize the terminal guanidino nitrogen atoms of precursor L-arginine to form NO *in vivo* and at the same time, L-citrulline is generated as a by-product. NO synthases contain heme and have binding sites for calcium and NADPH as well as L-arginine. NAPDH is one of the essential cofactors during NO production *in vivo.* Increases in calcium occur in endothelial cells stimulated by agonists such as acetylcholine and physical stimuli such as shear stress [Moncada *et al.,* 1991]. In resting platelets the synthesis of NO is not detectable, whereas NO synthase becomes activated during platelet aggregation leading to the formation of NO [Radomski et al., 1990a, 1990b]. The activation of the NO/L-arginine pathway may be attributed to the increase of intracellular calcium and is suggested to provide a means to limit the aggregation response.

EDRF was originally defined in terms of its ability to relax vascular tissue, although later it has been shown that EDRF/NO is involved in numerous physiological processes such as vasodilation, inhibition of platelet adhesion and aggregation, immune defense, neuroprotection, peristalsis, penile erection, and various endocrine and exocrine secretions in the cardiovascular, reproductive, and immune systems [Shinde *et al.,* 2000]. The mechanism of NO in the cardiovascular system functions as an inhibitor of platelet adhesion and aggregation is discussed.

Unlike prostacyclin, NO inhibitory actions on platelets occurs in a cyclic guanosine 3', 5'-monophosphate (cGMP)-dependent mechanism [Mellion *et al.,* 1981].

Under physiological conditions, NO has a high binding affinity for heme iron and therefore reacts with heme proteins including the soluble guanylate cyclase (SGC). This binding results in the activation of SGC, which converts guanosine 5'- triphosphate (GTP) into cGMP. The generated cGMP then stimulates cGMP-dependent protein kinase, which then phosphorylates specific proteins. The subsequent signal transduction remains to be unclear. The consequences resulting from enzyme phosphorylation due to cGMP-dependent kinase include the inhibition of collagen and finbrinogen binding to their receptor, inhibition of protein kinase C and IP3, modulation of phospholipase A_2- and C-induced responses, and sequestration of intracellular Ca^{2+} [Radomski and Moncada, 1993]. Furthermore, the elevated intracellular cGMP can crossover to increase intracellular cAMP by inhibiting the hydrolysis of cAMP by cyclic nucleotide phosphodiesterase (PDE) [Grand and Colman, 1984]. Thus, NO-mediated increases in cGMP can also promote the cAMP-dependent inhibition of platelet aggregation. Figure 2.8 illustrates the intracellular signal transduction via which NO release from endothelial cells functions as an inhibitor of platelet adhesion, activation, and aggregation.

Interestingly, only NO, not prostacyclin, plays a major role in preventing platelet adhesion. The adhesion of both thrombin-stimulated and unstimulated platelets onto endothelial cells was inhibited in the presence of exogenous NO or bradykinin which catalyzes prostacyclin and NO release from endothelial cells [Radomski *et al.,* 1987b]. The effect of bradykinin is not altered by aspirin, which suppresses platelet cyclooxygenase and thus inhibits prostacyclin release [Frolich, 1992]. However, bradykinin-induced inhibition of adhesion to endothelial cells is inhibited by hemoglobin,
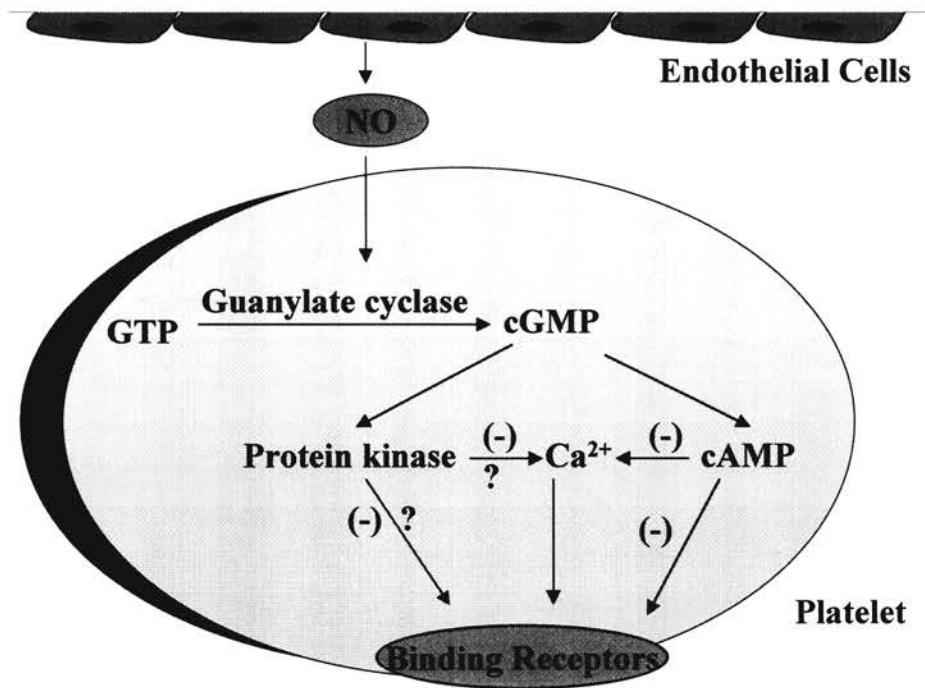
Figure 2.8. A schematic signal transduction pathway of the role of NO released from endothelial cells in inhibiting platelet adhesion, activation, and aggregation *in vivo*. (-) means the inhibition effect. ? means that the mechanism is unknown.

an agent known to scavenge NO [Sneddon and Vane, 1988]. These results show that NO, not prostacyclin, released from endothelial cells due to the stimulation of bradykinin is responsible for inhibiting platelet adhesion. It was also reported that platelet adhesion to fibrillar collagen is inhibited completely by NO but only partially by prostacyclin [Radomski *et al.*, 1987c]. In this sense, NO is the most potent inhibitor of platelet aggregation and thrombus formation since only NO can effectively inhibit platelet adhesion, the initial step of the cascade reactions of hemostasis.

2.3 The chemistry and physiology of S-nitrosothiols

As described in the above section, NO is a messenger molecule involving many physiological processes including smooth muscle relaxation and neurotransmission as well as inhibition of platelet adhesion and aggregation. However, the rapidity of NO reactions with molecular oxygen or superoxide anion to form toxic oxidizing agents (ntirogen dioxide and peroxynitrite, respectively) and its reaction with heme and nonheme iron definitely interferes with, or limits, the beneficial actions of NO on target tissues. Endogenous metabolites of NO, S-nitrosothiols (especially S-nitroso-proteins), have been detected in extra- and intracellular fluids and are considered as a NO reservoir to facilitate NO transport, prolong its life in the blood and tissue, target its delivery to specific effector sites, and mitigate its adverse cytotoxic potential [Fehel et al., 1996; Buzard and Kasprzak, *et al.*, 2000].

2.3.1 Chemical Properties of S-nitrosothiols.

Synthesis. Aqueous solutions of almost all nitrosothiols can be readily prepared by mixing thiol and acidified nitrite according to the following equations:

$$HNO_2 \;+\; H^+ \;\rightarrow\; NO^+ \;+\; H_2O \qquad (2.1)$$

$$RSH \;+\; NO^+ \;\rightarrow\; RSNO \;+\; H^+ \qquad (2.2)$$
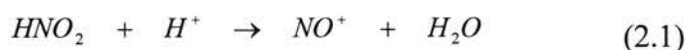
where RSH represents a thiol and RSNO S-nitrosothiol. Under some circumstances, these reactions usually is very rapid [Stamler and Loscalzo, 1992]. For example, RSANO is formed quantitatively within a minute when the corresponding thiol and sodium nitrite solutions both at a concentration of 10 mM are mixed in acid solution with

50 mM HCl [William, 1996]. This method is dominantly employed in the literature to prepare S-nitrosothiols for *in vitro* and *in vivo* experiments [Stamler *et al.*, 1992a; Keaney *et al.*, 1993; Mathews and Kerr, 1993; Liu *et al.*, 1998]. Nitrosation of thiols with NO gas in the liquid solution at neutral pH requires the presence of oxygen *in vitro*, which is carried out according to the following reaction scheme [Ignarro et al., 1993; Lewis and Deen, 1994; Wink et al., 1994].

$$2\,NO + O_2 \rightarrow 2\,NO_2 \qquad\qquad (2.3)$$

$$NO + NO_2 \Leftrightarrow N_2O_3 \qquad\qquad (2.4)$$

$$N_2O_3 + RSH \rightarrow RSNO + NO_2^- + H^+ \qquad\qquad (2.5)$$
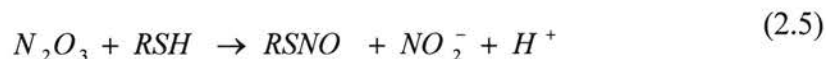
The above reaction mechanism may serve as one pathway for S-nitrosothiols formation *in vivo* although no direct evidence is provided so far. It was also reported that peroxynitrite may nitrosate, in part, tissue thiols such as glutathione [Wu *et al.*, 1994, van der Vliet *et al.*, 1998], which may help rationalize the high concentrations of S-nitrosothiols produced with inflammation [Gaston et al., 1993]. The reaction mechanism is suggested as follows

$$GSH + ONOOH \rightarrow GSNO + H_2O_2 \qquad\qquad (2.6)$$

Gow *et al.* (1997) proposed a different and novel reaction mechanism for the formatation of S-nitrosothiols *in vivo*, in which NO reacts directly with reduced thiols to produce a radical intermediate, R-S-NO-H. The intermediate then reduces an available electron acceptor to produce a RSNO. Under aerobic conditions, O_2 acts as the electron acceptor and is reduced to superoxide, which then reacts at a diffusion-limited rate with NO to form peroxynitrite (Eq. 2.7-2.9).

$$RSH \quad + \quad NO \quad \Leftrightarrow \quad RSNOH \tag{2.7}$$

$$RSNOH \quad + O_2 \rightarrow \quad RSNO \quad + H^+ + O_2^- \tag{2.8}$$

$$O_2^- + \quad NO \quad \rightarrow \quad ONOO^- \tag{2.9}$$
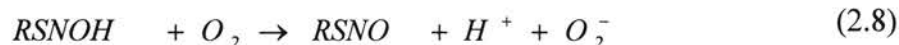
Therefore, RSNO can be formed *in vivo* under a wide variety of physiological and pathophysiological conditions although the specific formation pathways are still unclear.

Generally, S-nitrosothiols with tertiary structures such as S-nitroso-N-acetyle penicillamine (SNAP) are purple/green and ones with primary structures (e.g., glutathione) may vary from orange to red. S-nitrosothiols have relatively large extinction large coefficients in the 330-350 nm range, which is beneficial for monitoring the disappearance of nitrosothiols in quantitative studies. The specific extinction coefficients ($mM^{-1} \, cm^{-1}$) at 334 nm for some S-nitrosothiols are: 0.74 for S-nitroscysteine (CysNO), 0.73 for S-nitrosohomocysteine, 1.00 for SNAP, 0.87 for S-nitroso-N-acetyl-cysteine (SNAC), 0.85 for S-nitrosglutathione (GSNO), and 0.87 for S-nitrosoalbumin (AlbSNO) [Gordge *et al.*, 1996].

Stability. The stability of S-nitrosothiols has been the result of much confusion due to the fact that the presence of trace contaminating metal ions (specifically copper and mercury) enhances their degradation [Williams, 1996]. Consequently, the published half lives for S-nitrosothiols are sporadic due to the water purity difference from one lab to another.

Mathews and Kerr reported that half-lives of S-nitrosothiols in 0.5 mM HEPES-buffered physiological saline solution are 0.83 s for CySNO, 1.15 hr for SNAP, and 159 hr for GSNO at pH 7.4 and 37 °C (without chelator). However, the half-life of CysNO is about 30 s in physiological solution according to the data published by Myers et al.

(1994). Pietraforte et al. (1995) showed that BSANO is very stable in PBS at 37 °C in the absence of a chelator. Scorza et al. (1996) observed no NO release, within 3 hr, from BSANO and GSNO in N-ethylmaleimide (NEM)-treated dialyzed human plasma diluted to 50% (v/v) in PBS containing 0.1 mM DTPA. NEM treatment is used to remove the free thiol in the plasma and DTPA, as a chelator, was added to remove metal ions. Arnelle and Stamler (1995) showed that the half-lives are 60 min for CysNO, 2.7 hr for GSNO, and >10 hr for BSANO in 100 mM phosphate buffer (pH 7.4) containing 0.1 mM EDTA. Thus, the stability decreases in the order BSANO>GSNO>SNAP>CysNO in the same environment whether it contains metal ions chelators or not. Further, S-nitroso-proteins are often more stable than the S-nitroso derivatives of amino acids and small peptides [Stamler *et al.*, 1992a].

In addition to metals, light, pH, and temperature are also factors that influence the stability of S-nitrosothiols [Williams, 1996; Butler and Rhodes, 1997]. S-nitrosothiols should be stored in the dark if they are used for pharmacological studies although room light usually has little impact on the stability of S-nitrosothiols [Hogg, 2000]. S-nitrosothiols are usually prepared fresh and samples are kept in ice and away from light. Since S-nitrosothiols are very stable at low pH [Williams, 1996], some investigators also like to keep S-nitrosothiols in the acidic solution and then neutralize the solution prior to use.

2.3.2 Biological reactions of S-nitrosothiols

The physiological functions of S-nitroso-thiols are executed mainly by two reactions: NO release (degradation) and transnitrosation.

Degradation. In the presence of metal ions such as copper [Williams, 1996; Singh *et al.,* 1996; Stubauer *et al.,* 1999], iron [Vanin et al., 1997], and mercury [Williams, 1996], S-nitrosothiols are catalytically decomposed to yield the corresponding disulfide and NO. The generated NO is immediately converted into nitrite ion in the presence of oxygen [Lewis and Deen, 1994]. The mechanism of NO release from S-nitrosothiols due to catalysis of copper(II) has been fairly well established and is summarized by Eq. 2.10-2.11.

$$RS^- + Cu^{2+} \rightarrow RS \cdot + Cu^+ \tag{2.10}$$

$$RSNO + Cu^+ \rightarrow RS^- + Cu^{2+} \tag{2.11}$$

$$2\,RS \cdot \rightarrow RSSR \tag{2.12}$$

The first reaction can be initialized by thiol impurities present in the S-nitrosothiol sample or directly by S-nitrosothiol itself. However, copper (II) is so effective that a low contamination level (< 1 μM) is sufficient to cause NO release from S-nitrosothiols. GSNO is exceptional and only partially degraded in the presence of trace amounts of copper(II) since the disulfide GSSG formed due to degradation can rapidly chelate copper (II) [Hogg, 2000]. Neocuproine, a specific chelating agent for copper(I) [Yoshida *et al.,* 1994], can effectively inhibit the degradation of S-nitrosothiols [Williams, 1996]. This evidence supports that copper(I) is the true metal ion which catalyzes NO release according to Eq. 2.11.

In the presence of reducing agents (e.g., ascorbate and thiol), copper(II) is reduced to copper(I) which then reduces S-nitrosothiols (RSNO) to form a thiolate anion (RS$^-$) and NO [Kashiba-Iwatsuki *et al.,* 1996; Scorza *et al.,* 1997]. Scorza demonstrated that

the amount of thiol formed, the loss of GSNO, and NO released were almost the same when 200 μM GSNO was incubated in phosphate buffer saline (PBS) with 100 μM ascorbate at 37 °C. This evidence illustrates that NO release from S-nitrosthiols leads to the formation of free sulfhydryl in the presence of reducing agents. Scorza also observed that 100 μM human serum albumin (HSA) strongly promoted NO release from GSNO at the same conditions as ascorbate did. Since S-nitrosated HSA is much more stable than GSNO, HSA functioned through reducing copper(II) to copper(I) with its cysteine residue instead of through S-transnitrosation. In addition, superoxide, another *in vivo* agent, can also promote NO release from GSNO [Aleryani *et al.,* 1998; Jourd'heuil *et al.,* 1998].

In addition to the metal ion-catalyzed route, both photolytic and thermal pathways can cause the degradation of S-nitrosothiols to form a disulfide and NO (Eq. 2.13). Sexton *et al.* (1994) showed that NO was released when GSNO was irradiated at either 340 tor 545 nm (the absorption wavelengths of GSNO). The photolytic release of NO enhanced the cytotoxic effects of GSNO on leukemia cells, raising possibility that GSNO and other S-nitrosothiols may be used as photochemotherapeutic agents. Singh *et al.,* (1995) described a quantitative method how to trap and measure NO released from S-nitrosothiols due to photolytic decomposition.

$$2\,RSNO \xrightarrow{\quad \Delta\ or\ h\nu \quad} RSSR + 2\,NO \qquad (2.13)$$
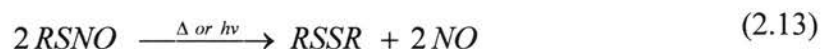
Transnitrosation. Transnitrosation is defined as the transfer of a NO moiety from a S-nitrosothiol (RSNO) to a thiol in exchange for an H moiety [Feelisch, 1991]. The reaction scheme is expressed as follows.

$$RSNO + R'SH \rightarrow RSH + R'SNO \qquad\qquad (2.14)$$

This reaction occurs *in vitro* and is reversible [Hogg, 1999], which is considered as one of the mechanisms for the generation of S-nitrosothiols *in vivo*. Scharfstein *et al.* (1994) demonstrated that NO bound to protein thiols (albumin) was significantly transferred to low molecular-weight thiols (L-cysteine and N-acetyle-L-cysteine) *in vivo*. Table 2.1 lists some reported reaction rate and equilibrium constants for transnitrosation. The rate constants measured are highly dependable on the methods used. The forward rate constants were usually determined using either pseudo-first-order conditions or initial rates [Meyer *et al.*, 1994; Singh, 1996]. Both methodologies are problematic because the pseudo-first-order approximation is not applicable to second-order reversible reactions and approximation of a tangent to the initial rate is error-prone. In addition, the method of separately detecting two S-nitrosothiols in the same solution is not available to date, which limits the precision of rate constants. Despite the data inconsistencies, the following conclusions can be drawn from Table 2.1.

- The equilibrium constant between albSNO (including BSANO and AlbSNO) and CySH is close to unity.

- NO moiety in albSNO is more likely transferred to CySH than GSH according to Meyer *et al.*, 1994.

- Transnitrosation between albSNO and CySH is fast and the forward reaction rate is as high as 9.1 $M^{-1} s^{-1}$.

Table 2.1

Rate constants for transnitrosation reactions between S-nitrosothiols and thiols

RSNO	R'SH	k_f (M^{-1} s^{-1})	k_r (M^{-1} s^{-1})	K_{eq}	References
GSNO	CySH	139 ± 12	675 ± 254	0.2	Hogg, 1999
				0.35	Singh *et al.*, 1996
				0.53	Tsikas *et al.*, 1999
			57		Rossi *et al.*, 1997
		71	88	0.83	Meyer et al., 1994
	hCySH	35.0 ± 3.8	13.7 ± 4.4	2.54	Hogg, 1999
				2.09	Tsikas *et al.*, 1999
SNAP	GSH	5.39 ± 0.47	1.72 ± 0.35	3.69	Hogg, 1999
		9.09 ± 0.78	0.53 ± 0.13	18.6	Singh *et al.*, 1996
				6.67	Tsikas *et al.*, 1999
		1.17	0.9	1.7	Meyer et al., 1994
	CySH	20.6 ± 3.2	3.15 ± 1.11	6.46	Singh *et al.*, 1996
				2.89	Tsikas *et al.*, 1999
		3.1	1.3	2.38	Meyer et al., 1994
	hCySH			1.22	Tsikas *et al.*, 1999
SNAC	GSH			0.35	Tsikas *et al.*, 1999
			27		Rossi *et al.*, 1997
	CySH			0.20	Tsikas *et al.*, 1999
	hCySH			1.22	Tsikas *et al.*, 1999
albSNO	GSH	19.0 ± 2.1	159 ± 26.2	0.12	Hogg, 1999
				0.59	Tsikas *et al.*, 1999
			5.78		Rossi *et al.*, 1997
			13		Zhang *et al.*, 1996
		3.2			Meyer et al., 1994
albSNO	CySH			0.75	Tsikas *et al.*, 1999
			52		Zhang *et al.*, 1996
		9.1			Meyer et al., 1994

Abbreviations: GSNO, S-nitrosoglutathione; GSH, glutathione; SNAP, S-nitroso-N-acetylpenicillamine; SNAC, S-nitroso-N-acetylcyssteine; albSNO, S-nitroso-bovine serum albumin or S-nitroso-human albumin; CySH, L-cysteine; hCySH, homocysteine; k_f, forward reaction rate constant; k_v, reverse reaction rate constant; K_{eq}, equilibrium constant.

The above observations provide an important clue for developing the concept of using endogenous NO to improve the haemocompatibility of existing biomaterials, which will be discussed in Section 2.4.

2.3.3 Biological activities of S-nitrosothiols

S-nitrosothiols occurs naturally in plasma and other body fluids. Stamler *et al.* (1992b) initially reported that the concentration of S-nitroso-proteins in human plasma is as high as 7 μM, of which ~ 6 μM is S-nitroso-human serum albumin (AlbNO), according to a detection system based on UV-photolytic cleavage of the -S-NO bond. More recently, it has been reported that the AlbNO concentration in human plasma is ~0.22 μM using HPLC analysis [Goldman *et al.*, 1998] and ~0.20 μM using GC analysis [Tsikas *et al.*, 1999], respectively. S-nitrosothiols, predominantly as GSNO, were detected at 0.2-0.5 μM concentrations in human alveolar fluid [Gaston *et al.*, 1993].

Interestingly, the biological activities of S-nitrosothiols were realized before the landmark discovery that NO was an endogenously generated molecule. S-nitrosothiol inhibitory effects on bacterial growth (e.g., *Bacillus cereus*) were well studied during 1970s and early 1980s [Incze *et al.*, 1974; Kanner *et al.*, 1979; Morris and Hansen, 1981]. Ignarro and coworkers first demonstrated that S-nitrosothiols activated guanylate cyclase and relaxed coronary arterial smooth muscle as intermediates in the metabolism of drugs such as glyceryl trinitrate and nitroprusside [Ingarro *et al.*, 1980; Ingarro *et al.*, 1980; Gruetter *et al.*, 1980; Gruetter *et al.*, 1981]. It was not until 1987 that NO was identified as EDRF [Palmer *et al.*, 1987]. A number of S-nitrosothiols including CySNO and GSNO have been shown to possess vasodilatory activity as well as the ability to inhibit

platelet aggregation. Both of these functions are usually attributed to NO release. However, there is some evidence that S-nitrosothiols can exhibit direct effects in some locations that makes it functionally distinct form endogenous NO [Kowaluk and Fung, 1990]. Later, Mathews and Kerr (1993) reported similar results using a wide range of S-nitrosothiols in both vessel relaxation and platelet aggregation studies. Both studies implied that extracellular effects might be responsible for the activity of S-nitrosothiols since intracellular penetration is not observed. The evidence provided by Gordge et al. (1996) supports that GSNO exerts its antiplatelet action via a copper-dependent membrane enzyme, rather than spontaneous release of NO. These observations highlighted that NO release is unnecessary for the antiplatelet and vasodilatory activities of S-nitrosothiols. However, co-incubation with copper (II) [de Man *et al.*, 1996] or in the presence of thiol [Gordge *et al.*, 1996] or ascorbate [de Man *et al.*, 1998] can enhance the biological functions of S-nitrosothiols, which demonstrated that catalytic NO release is beneficial for the performance of S-nitrosothiols.

S-nitrosation of many enzymes has been observed and the chemical modification usually leads to the modification of the activities. NO species can trigger and activate intracellular intermediary signaling kinases [Lander *et al.*, 1996]. S-nitrosylation of the nuclear protein transcription factors p50, c-jun, and c-Myb on DNA binding resulted in significantly decreased DNA binding, which may account for the function of NO in gene transcription [Brendeford *et al.*, 1998; dela Torre *et al.*, 1998]. Other examples that S-nitrosation is implicated in the control of enzyme activity include activation of N-methyle-D-asparate receptor-channel complex [Lei *et al.*, 1992], Ca^{2+}-acitvated K^+ channels [Bolotina et al., 1994], cyclic nucleotide-gated (CNG) channels [Broillet and

43

Firestein, 1997], Na$^+$ channels in baroreceptors [Li *et al.*, 1998], cardiac Ca^{2+} release channels [Xu *et al.*, 1998], inhibition of adenosyltransferase [Ruiz et al., 1998], glutathione-S-transferases [Clark and Debnam, 1988], and plasma clotting factor XIII [Catani *et al.*, 1998].

More interestingly, Persichini *et al.* (1998) found that cysteine nitrosation inactivates the human immunodeficiency virus (HIV)-1 protease. HIV-protease action is modulated by the redox equilibrium of Cys678 and Cys95 regulatory residues. Thus HIV-1 protease inactivation via NO-mediated nitrosation of CySH regulatory residues may represent an interesting possible mechanism for inhibition of HIV-1 replication and an indication that S-nitrosylation modulates the catalytic activity of cysteine-containing enzymes. One year later, Persichini *et al.* (1999) published that NO can inhibit HIV-1 replication in human astrocytoma cells.

S-nitrosation of protein may also regulate apoptosis. A family of proteases collectively known as caspases has been implicated as a common executor of a variety of death signals. Tenneti et al. (1997), Li et al. (1997), and Haendeler et al. (1998) have shown that each member of the caspase family, which participates in apoptotic signal transduction and execution mechansims, contains a critical cysteine residue in its active site and that S-nitrosation of caspases on this particular cysteine residue decreases enzyme activity and is associated with protection from apoptosis. These studies suggested that low concentrations of NO may inhibit the cellular suicide program via nitrosation of members of the caspase family.

The detection of S-nitrosohemoglobin (SNO-Hb) in human circulation engendered the hypothesis that S-nitrosation may also play a role in modulating oxygen

transport [Jia *et al.,* 1996]. Electrospray mass spectrometry has revealed a single S-nitroso group on β93 cysteine of hemoglobin (Hb) exposed to CySNO [Ferranti *et al.,* 1997]. Stamler et al. (1997) found that the binding of oxygen to heme irons in Hb promotes the formation of SNO-Hb. Deoxygenation is accompanied by an allosteric transition in SNO-Hb from the R(oxygenated) to the T(deoxygenated) structure that releases the NO group. SNO-Hb is a vasoconstrictor in 95% oxygen but in <1% its vasoconstrictive effects are converted into vasodilatory effects. By sensing the physiological oxygen gradient in tissues, SNO-Hb can release NO to bring local blood flow into line with oxygen requirements.

2.4 The rationale for improving the haemocompatibility of blood contacting via endogenous NO

In Chapter 1, it is discussed that the haemocompatibility of biomaterials is still a concern since existing biomaterials may generate several potential side-effects on patients as well as reduce the performance of blood-contacting medical devices. Also the disadvantages and advantages were discussed about the current methods that have been studied to solve the thrombogenicity of existing biomaterials, in which NO release polymers are emphasized. Although NO release polymers are very promising since localized NO release may be the most effective antiplatelet agent as discussed in Section 2.2.3, some disadvantages (e.g., non-constant release rate and short life) limit their applications. The core of this thesis is to advance and demonstrate the novel idea that the haemocompatibility of blood-contacting polymers can be alternatively improved by exploiting endogenous NO. The rationale for the novel process is discussed below.

a) *Abundant endogenous NO exists in human blood.*

Human blood plasma contains endogenous NO bound to proteins (S-nitroso-proteins), mostly as S-nitrosoalbumin (AlbSNO). Stamler *et al.* (1992) initially reported that S-nitrosoproteins in plasma are ~7 µM, of which ~6 µM is AlbSNO. The value of AlbSNO measured by HPLC [Goldman *et al.*, 1998] and GC [Tsikas *et al.*, 1999] is ~0.22 µM and 0.20 µM, respectively. Although the later values are one order of magnitude lower than that reported by Stamler *et al.*, AlbSNO is still a significant concentration in plasma. However, NO bound to albumin is not available for the rapid need of blood-contacting polymers because it is the most stable S-nitrosothiol as discussed in Section 2.3.1.

More specifically, the time course of the release of NO from S-nitroso-albumin in plasma was demonstrated to be identical regardless of whether BSANO (bovine) or AlbSNO (human) was used [Scorza et al., 1996]; Pietraforte *et al.* (1995) observed that within 1 hr NO was not released from BSANO when it was incubated in phosphate-buffered saline (pH 7.4) at 37 °C; Similarly, Scorza *et al.* (1996) reported that BSANO did not release NO within 3 hr in NEM-treated dialyzed plasma at 37 °C and only ~10% BSANO was decomposed within 3 hr if BSANO was incubated in untreated human plasma. Therefore, NO bound to proteins in human plasma would not spontaneously and automatically released to inhibit platelet adhesion and aggregation on the foreign surface of biomaterials if such thrombogenic polymers were used in blood-contacting medical devices.

b) *Spontaneous transnitrosation exists between S-nitroso-albumin and L-cysteine*

A fast and spontaneous transnitrosation (Eq. 2. 14) exists between S-nitroso-albumin including human and bovine albumin and low molecular weight thiols (e. g., L-cysteine and glutathione) as presented in Section 2.3.2. Since AlbSNO and BSANO have similar NO release properties and both are S-nitroso-serum albumin proteins, it may be assumed both AlbSNO and BSANO have the same properties of transnitrosation with low molecule thiols. Most investigators used BSANO to study the kinetics between S-nitroso-albumin and low molecular weight thiols because the commercial bovine serum albumin is less expensive than human serum albumin, which is also the reason why BSANO is used in the later experiment in this thesis.

$$albSNO + CySH \Leftrightarrow albSH + CySNO \qquad (2.14)$$
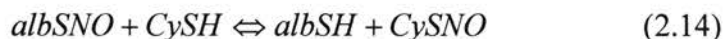
The forward rate constant of transnitrosation between AlbSNO (human) and L-cysteine is ~ 9.2 M^{-1} s^{-1} as measured by Meyer et al. (1994). Additionally, the NO transfer from BSANO to L-cysteine is faster than NO transfer to other low molecular thiols such as glutathione according to the data listed in Table 2.1. It also has been shown that NO can be transfer to L-cysteine from BSANO *in vivo* [Scharfstein *et al.*, 1994].

c) *S-nitroso-L-cysteine (CySNO) is the most unstable S-nitrosothiol*

As discussed in Section 2.3.1, nitrosated high molecular weight thiols such as BSANO are much more stable than nitrosated low molecular weight thiols, in which CysNO is the most unstable S-nitrosothiol although its stability strongly depends on factors such as metal ions, pH, and temperature. One study showed that the half-life of CysNO is almost similar to NO and is as short as ~ 30 sec at physiological conditions [Myer *et al.*, 1990]. It is well known that CysNO decomposes to yield the corresponding disulfide and the release of NO if no other reducing agents exist as discussed in Section 2.3.2. However, the decomposition of CysNO may form NO and reduced L-cysteine if other reducing agents (e. g., thiols and ascorbate) are present to reduce Cu^{2+} to Cu^{+} (Eq. 2.15) [Williams, 1996; Stubauer et al., 1999; Hogg, 2000].

$$CySNO + H^{+} \xrightarrow{Cu^{+} \to Cu^{2+}} CySH + NO \uparrow \qquad (2.15)$$

d) *Free L-cysteine catalyzes NO release from BSANO*

It has been demonstrated that free L-cysteine, through transnitrosation, can catalyze NO release from albSNO (including AlbSNO and BSANO). The experiments performed by Meyer *et al.* (1994) showed that 0.2 mM AlbSNO dramatically decreased to 0.05 mM within 1 min by L-cysteine in the presence of cupric sulphate at 37 °C and pH 7.4. Pietraforte *et al.* (1995) reported that L-cysteine enhanced, through transnitrosation, NO release from BSANO in phosphate buffer (pH 7.4) at 37 °C and the half-life of BSANO was about 15 min in the presence of equimolar amounts of L-cysteine. However, BSANO did not degrade within 1 hr in the absence of L-cysteine. Scorza et al. (1997) tested the effect of L-cysteine on the stability of BSANO in dialyzed human plasma at 37 °C and pH 7.4. The experimental results also illustrated that as low as 10 μM L-cysteine significantly catalyzed NO release from BSANO in comparison with control. In addition, Gordge et al. (1996) observed that the release rate of NO from BSANO was dramatically increased from ~0.19 nmol·min^{-1} to ~1.52 nmol·min^{-1} in the presence of free L-cysteine and the biological activity of BSANO (e. g., inhibiting platelet aggregation) was also significantly enhanced in the presence of L-cysteine.

According to the above investigations, we proposed a novel idea of exploiting endogenous NO present in human blood to improve the haemocompatibility of blood-contacting polymers as illustrated in Figure 2.9. First, L-cysteine is attached to the blood-contacting surface of polymers. When blood flows over a L-cysteine-modified surface, the immobilized L-cysteine with a free thiol group is able to extract NO from AlbSNO in human plasma via S-transnitrosation. Then, CySNO formed following
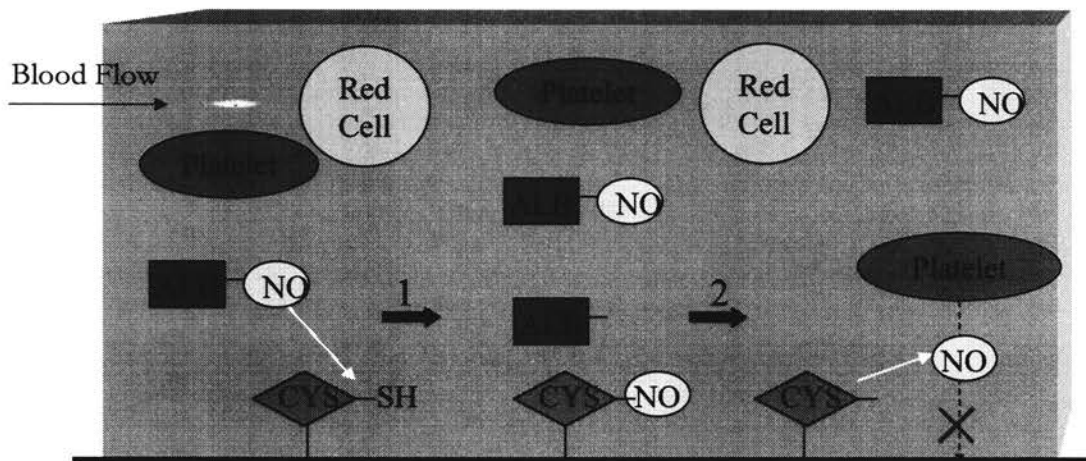
Figure 2.9. Mechanism of inhibiting platelet adhesion onto biomaterials by exploiting endogenous nitric oxide. 1. S-transnitrosation: NO bound to albumin is transferred to L-cysteine immobilized on the surface. 2. Decomposition: NO is spontaneously released from unstable CySNO to inhibit platelet adhesion.

transnitrosation quickly releases NO from the surface under the catalysis of ascorbate or/and copper, or other reducing thiols and copper. Finally, NO release inhibits platelet adhesion, aggregation, and thrombus formation. Therefore, the haemocompatibility issue of existing biomaterials would no long complicate patients and blood-contacting medical devices.

It is noteworthy whether CySNO formed following S-transnitrosation decomposes to form disulfide (cystine) or L-cysteine. Normally, human plasma contains ~50 μM ascorbate [Menditto *et al.*, 1992], 20 μM copper [Reyes et al., 2000], and ~ 5 μM glutathione [Aebi *et al.*, 1991; Kleinman and Riche, 2000]. As discussed in Section 2.3.3, Kashiba-Iwatsuki *et al.* (1996) and Scorza *et al.* (1997) reported that S-nitrosothiol decomposition resulted in the formation of the reduced thiols and NO in the presence of ascorbate, which may be due to the mechanism that ascorbate reduce copper (II) to copper(I), after which copper (I) catalyze NsO release from S-nitrosothiols according to the Eq. 2.15. Alternatively, glutathione has a negative redox potential and can easily reduce copper (II) to copper (I) to promote the formation of reduced L-cysteine and NO. Therefore, it is highly possible that CySNO decomposition on the surface will form L-cysteine that can continually be utilized for transnitrosation and NO release although this needs to be further investigated.

The advantages of this method are obvious in comparison with NO release polymers. First, this method does not introduce exogenous NO into patients since exogenous NO has the potential to lead to cytotoxic and mutagenic effects [Hibbs *et al.*, 1987; Tamir *et al.*, 1996; Keshive *et al.*, 1996; Fehsel *et al.*, 1996]. Second, the NO release rate would be controlled to a certain value by attaching an appropriate amount of

L-cysteine on the surface. This would be beneficial if the NO release rate is lower than the threshold for causing toxic effects and at the same time higher to effectively inhibit platelet adhesion. Third, NO release would be permanent, instead of several hours to couples of weeks with current NO release polymers. In this sense, this method may be used for long-term applications of biomaterials (e.g., vascular grafts) as well as short-term applications. Fourth, this method may avoid the toxic concerns from NO donor residues in NO-releasing polymers as well as change of polymer properties. As discussed in Chapter 1, NO donor residues may form carcinogenic nitrosamines once released from the polymer. Also biomaterial mechanical properties may be negatively altered after a NO donor is incorporate into the polymer.

In order to demonstrate that this novel idea is feasible, the following investigations have been performed:

In Chapter 3, different surface modification methods are explored to attach L-cysteine onto biomaterials. Polyurethane (PU) and polyethylene terephthalate (PET), two pivotal polymers used in blood-contacting medical devices, are successfully immobilized with L-cysteine using glutaraldehyde as a crosslinker after they are aminolyzed by 3-aminopropyltriethoxysilane (APTES) and ethylenediamine, respectively. A fluoresecent labeling assay qualitatively shows that L-cysteine is attached on the surface of the two polymers. In Chapter 4, a chemiluminescence-based assay is developed to precisely quantify the amount of L-cysteine immobilized on PU and PET.

In Chapter 5, *in vitro* experiments including stagnant and flow tests are performed to evaluate platelet adhesion on L-cysteine-modified polymers. The results show that L-cysteine-modified polymers inhibit platelet adhesion, compared with control, only in the

presence of S-nitroso-albumin. S-transnitrosation between BSANO and immobilized L-cysteine and NO release from CySNO formed following transnitrosation are monitored. The final results show that the mechanism proposed in Figure 2.9 is fully supported. Additionally, S-transnitrosation kinetics between BSANO and L-cysteine immobilized on PET are measured and the rate and equilibrium constants are calculated according to the experimental data.

In the last chapter, the entire work is summarized and some recommendations are made for the future experiments to apply this technology to practical medical devices.

CHAPTER 3

IMMOBILIZATION OF L-CYSTEINE ONTO POLYMERIC BIOMATERIALS

The objective of this thesis is to assess the hypothesis that L-cysteine-modified polymers can extract NO from endogenous S-nitrosoproteins through transnitrosation and then release NO through decomposition when exposed human blood. The NO release from L-cysteine-modified polymers will then be able to effectively inhibit platelet adhesion, activation, and aggregation. In order to test the hypothesis, L-cysteine must be immobilized onto polymeric biomaterials.

3.1 Methods for modifying the surfaces of materials

Biomolecules such as enzymes, antibodies, or drugs, as well as cells, have been immobilized onto the surface of polymeric biomaterials for a wide range of applications including improving blood compatibility, influencing cell adhesion and growth, controlling protein adsorption, modifying lubricity, and optimizing corrosion resistance [Ratner and Castner, 1997]. As described in Chapter 1, heparin, albumin, and poly(ethylene oxide) were immobilized onto polymers to improve the haemocompatibility. The rationale for the surface modification is obvious: to retain the key physical properties of the polymer while modifying only the outermost surface to influence the biointeraction. If polymer surface modifications are properly carried out,

the mechanical properties and functionality of the polymer will be unaffected, while improving biocompatibility. The methods to modify the surfaces of polymeric biomaterials are numerous and briefly described here.

Noncovalent coatings. Noncovalent coatings are physically based and, in many cases, used for the temporary localization of a biomolecule on the solid support. Solution coating a polymer is the simplest and most traditional form of noncovalent coating. Figure 3.1 illustrates schematically the Langmuir-Blodgett (LB) film deposition method which was studied extensively in the late 1980s [Bird *et al.*, 1989; Meller *et al.*, 1989; Cho *et al.*, 1990; Knobler, 1990]. The LB deposition method covers a surface with a highly ordered layer. The molecules that assemble into this layer contain a polar head group and a nonpolar region such as phospholipid and fatty acid. The advantages of this method are the high degree of order and uniformity. Also there are many options for incorporating new chemistries at surfaces since a variety of chemical structures can form LB films.

Self-assembled monolayers (SAMs) are surface-coating films that spontaneously form as highly ordered structures (two-dimensional crystals) on specific substrates (Ulman, 1991; Whitesides *et al.*, 1991). The important difference between SAMs and LB films is that SAMs occurs spontaneously and LB films only form with external help (such as pressure). Two processes are involved with the formation of SAMs: a strong adsorption of an anchoring chemical group to the surface and van der Waals interaction of the alkyl chains. The strong and exothermic binding to the surface provides a driving force to fill every site on the surface. Once every adsorption site is filled on the surface, the nonpolar region of the adsorbing molecule will be in sufficiently close proximity to

A

B

C
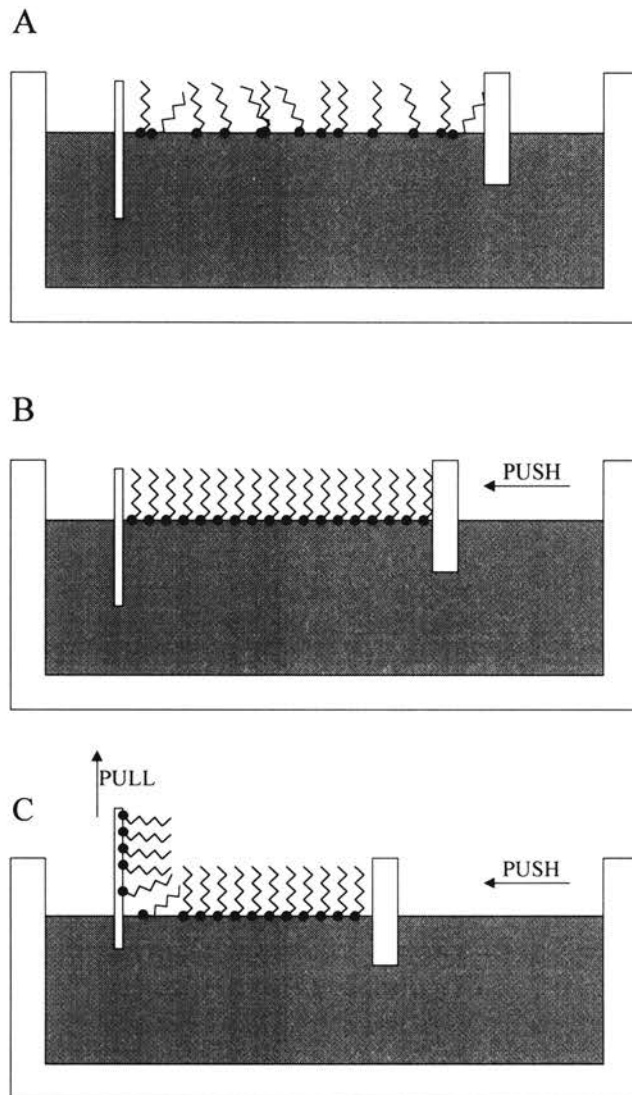
Figure 3.1. Deposition of a lipid film onto a glass slide by the Langmuir-Blodgett technique. A). The lipid film is floated on the water layer. B) The lipid film is compressed by a moveable barrier. C) The vertical glass slide is withdrawn while pressure is maintained on the floating lipid film with the movable barrier. The figure is adapted from Ratner and Hoffman, 1996.

each other so that van der Waals interactive forces between molecules lead to crystallization. Molecules that form SAMs have the general characteristics depicted in Figure 3.2. The advantages of SAMs are the easy formation and the higher stability as compared to LB films.

Noncovalent coatings also include surface-modifying additives (SMA), which means that certain compounds are added in low concentrations to a material during fabrication and spontaneously rise to and dominate the surface [Ward, 1989]. The driving force to concentrate the SMA at the surface is the reduction of the interfacial energy. A typical SMA designed to alter the surface properties of a polymeric material will be a relatively low-molecular-weight diblock copolymer. The "A" block will be soluble in, or compatible with, the bulk material into which SMA is being added. The "B" block will be incompatible with the bulk material and have a lower surface energy. Thus, the A block will anchor the B block into the material to be modified at the interface. During initial fabrication, the SMA might be distributed uniformly throughout the bulk and then migrate to the surface after a period for curing.

All the above noncovalent coating methods cannot form permanent and stable surface layers. For the experiments designed in this thesis, the desire is for L-cysteine to stay on the surface of the polymer and keep "extracting" NO and "releasing" NO. Therefore, both SAMs and SMA are not considered although they usually form more stable surfaces than LB deposition.

Functional head group
(e.g., -OH, HC=O)

Van Der Waals forces

Van Der Waals forces

Van Der Waals forces

Assembling structure (e.g., alkyl groups)

Attachment group (e.g., -COOH, silane)

Strong interactions

Substrate (e.g., silica, Al_2O_3)
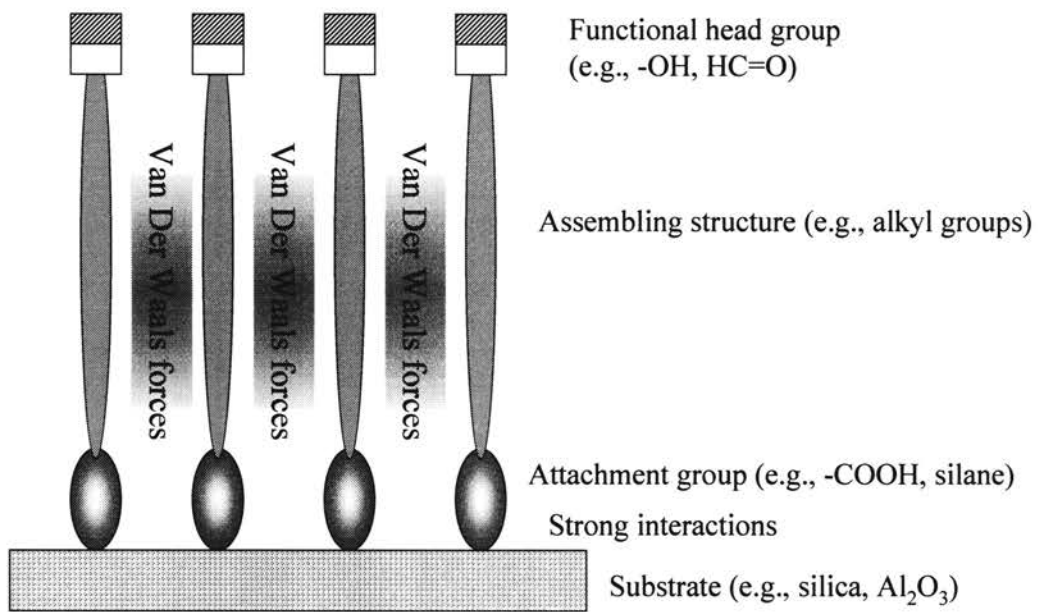
Figure 3.2. General characteristics of molecules that form self-assembled monolayers. Figure adapted from Ratner and Hoffman, 1996.

Covalently attached coatings. Radiation grafting and plasma (gas discharge) are two methods for covalently attached coatings. Radiation grafting has been widely used for the surface modification of biomaterials [Stannett, 1990], which include grafting using ionizing radiation sources (most commonly, a cobalt-60 gamma radiation source), grafting using UV radiation (Dunkirk *et al.,* 1991], and grafting using high-energy electron beams. In all cases, similar processes occur. The radiation breaks chemical bonds in the materials to be grafted, forming free radicals, peroxides, or other reactive species. These reactive surface groups are then exposed to a monomer. The monomer reacts with free radicals at the surface and propagates as a free radical chain reaction, incorporating other monomers into a surface-grafted polymer. Radiation grafting and photografting have frequently been used to bond hydrogels to the surfaces of hydrophobic polymers [Matsuda and Inoue, 1990; Dunkirk *et al.,* 1991]. The protein interactions, cell interactions, blood compatibility, and tissue reaction of hydrogel graft surfaces have been investigated [Hoffman *et al.,* 1983; Matsuda and Inoue, 1990].

Plasma deposition has often been used to introduce organic functional groups (e.g., amine, hydroxyl) on a polymer surface that can subsequently be treated by more conventional chemical derivation processes to attach biomolecules. Radio frequency glow discharges (RFGD) are low-pressure, non-equilibrium plasma techniques that have contributed to the production of new materials and devices in microelectronic and semiconductor industries [Sawin and Reif, 1983]. Now RFGD plasma surface modifications have been demonstrated to have special promise for the development of improved biomaterials, which is supported by the following features:

- The deposition forms void-free, well-adherent thin films (10-1,000 nm) of chemical composition and properties.

- The modification of the outermost surface layers can be fulfilled by grafting chemical groups or by inducing cross-linking and branching.

- Plasma-deposited polymeric films can be placed upon almost any solid substrate, including metals and ceramics.

- Plasma-treated surfaces are sterile when removed from the reactor, offering an additional advantage for cost-efficient production of medical devices.

The disadvantages of plasma deposition are also obvious. First, the chemistry produced on a surface usually is ill defined since numerous unwanted radicals are formed in the plasma reactor. Secondly, the apparatus used to produce plasma deposition is expensive and not available in many research labs. In addition, contamination can be a problem and care must be exercised to prevent extraneous gases.

Chemical reaction is the most widely used method to covalently attach functional biomolecules onto solid support surfaces. The layer of functional compounds deposited on solid supports by noncovalent coatings (including LB deposition and SAMs), in most cases, are not stable and some compounds are easily detached. The detachment is not desirable for most applications although it is preferable in some drug delivery systems. Radiation grafting, including plasma treatment, usually is employed to activate the inert surface of biomaterials for subsequent immobilization of functional biomolecules through chemical reaction. Hundreds of chemical reactions have been developed for covalent binding of biomolecules to solid polymeric supports. The reactions to an activated surface are summarized in Figure 3.3.

1) Pre-activation of support

Active support   Coupling agent
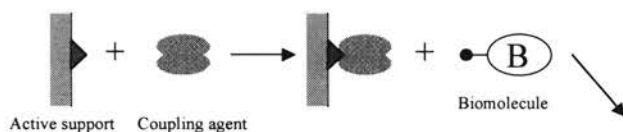
Biomolecule

2) Direct coupling to support

Polymer attached with
biomolecule via the
coupling agent
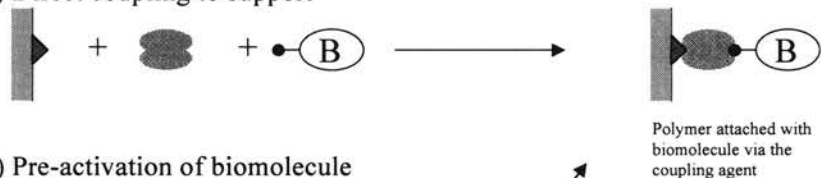
3) Pre-activation of biomolecule
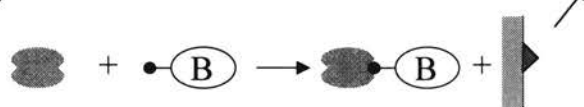
4) Conjugation followed by copolymerization

Comonomer   a) soluble copolymer

Activated
monomer

Crosslinker

b) Gel

Surface
radicals
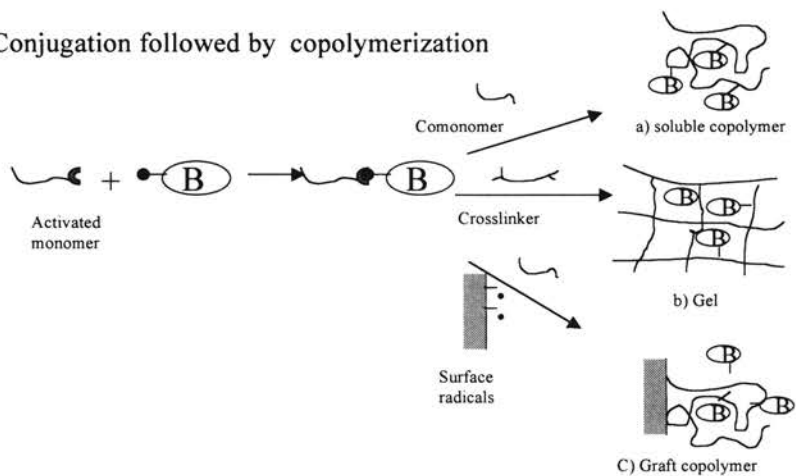
C) Graft copolymer

5) Direct attachment to pre-activated
   polymer, gel or grafted coplymer

Comonomer   Same as 4a

soluble copolymer

Crosslinker   Same as 4b

Gel

Surface
radicals   Same as 4c
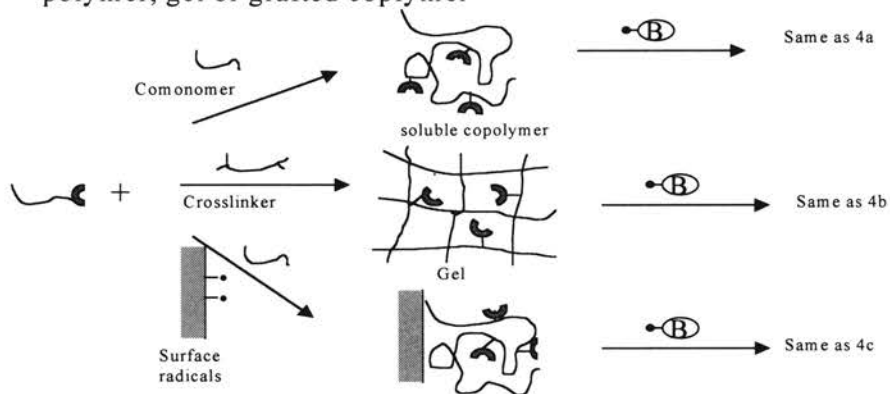
Figure 3.3. Schematic showing various methods for covalent biomolecule
immobilization. Figure adapted from Hoffman, 1996.

In some literature, the chemical linker is also called a spacer arm or leash, via which biomolecules are chemically immobilized. Most often the spacer arm reactive end groups are amine, carboxylic acid, aldehyde, and/or hydroxyl groups. Long spacer arms can provide greater steric freedom and thus greater specific activity for the immobilized biomolecule. For example, when affinity chromatography is used to separate a specific protein through attaching a corresponding ligand to the affinity matrix (e.g., Sephadex or Agarose), the spacer arm must be long enough to allow the interaction of ligand and protein.

Under the appropriate conditions, chemical reactions can be used to specifically immobilize biomolecules onto a support with a high yield and few side reactions. Normally, chemical reactions can easily be carried out in glassware and do not require expensive equipment. Compared with LB deposition and self-assembled monolayers, immobilization via chemical reaction can lead to covalent bonding of functional molecules on a solid support. Therefore, chemical reaction is the desired method to immobilize L-cysteine to blood-contacting polymers.

3.2 Selection of substrates and crosslinker

In this thesis, two pivotal blood-contacting polymers (polyurethane and polyethylene terephthalate (PET)) are selected as the substrates to which L-cysteine is attached. Polyurethane has rubber characteristics while PET is semicrystalline. The chemical structures of both polymers (actually copolymers) are shown in Figure 3.4. Both polymers possess relatively good blood compatibility, have good mechanical properties, and are chemically stable *in vivo* [Plank *et al.,* 1984; Bui and Thompson,

1993; Bernacca *et al.,* 1998].   The typical applications of polyurethane in humans include artificial heart ventricles, blood vessel prostheses, catheters, and heart assist pumps [Kang *et al.,* 1998].   PET is widely used in making woven vascular prostheses and heart valve suture rings [Kline, 1988].

Polyethylene terephthalate:

$$H{-}[{-}O{-}CH_2{-}CH_2{-}O{-}\underset{\underset{O}{\|}}{C}{-}\bigcirc{-}\underset{\underset{O}{\|}}{C}{-}]_n{-}OH$$

Polyurethane:

$$H{-}\,O{-}\,\{[{-}R_2{-}O{-}]_x[{-}\underset{\underset{O}{\|}}{C}{-}\,NH{-}R_1{-}NH{-}\underset{\underset{O}{\|}}{C}{-}]_y\}_n{-}O{-}R_2{-}OH$$

$$R_1: \;-\bigcirc{-}CH_2{-}\bigcirc{-}$$

$$R_2: -CH(CH_3)CH_2- \;\; or \;\; -(CH_2)_4-$$
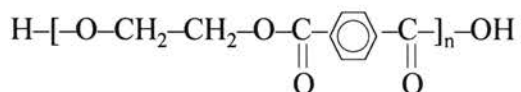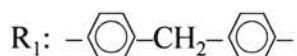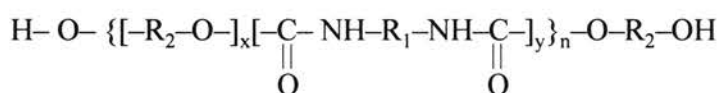
Figure 3.4 Chemical structure of polyurethane and polyethylene terephthalate

There are two reacting groups on L-cysteine which can be employed for immobilization: the primary amine ($-NH_2$) and the thiol (-SH). However, a free thiol is desired following the immobilization of L-cysteine so that NO can be "extract" from S-nitrosoproteins through transnitrosation and then released. Therefore, the amino group of L-cysteine is chosen as the reaction group for L-cysteine immobilization. Polyurethane and PET have inert surfaces and have to be chemically modified to provide reactive groups for immobilization. Both polymers are initially aminated so that glutaraldehyde can be utilized as a linker between the amino group of L-cysteine and the aminated surface.

63

Glutaraldehyde has been used more frequently as a cross-linking agent than any other reagent, since it is less expensive, is readily available, and is highly soluble in aqueous solution [Jayakrishnan and Jameela, 1996]. The aqueous solution of glutaraldehyde consist of free glutaraldehyde (a), cyclic hemiacetal (b), and oligomers (c), which are in equilibrium each other as illustrated in Figure 3.5.
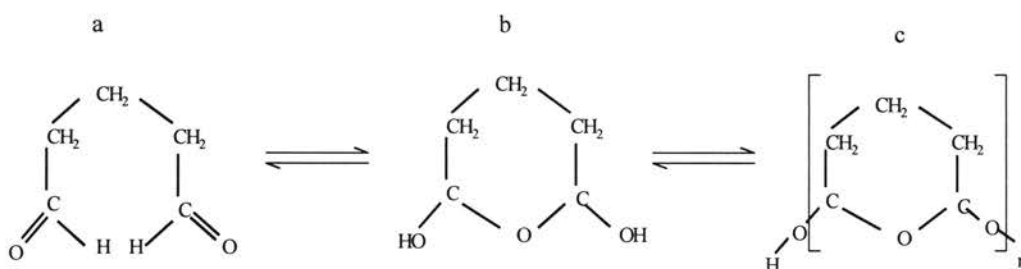
Figure 3.5. Equilibrium of the three forms of glutaraldehyde in aqueous solution.

Studies showed that polymerization of glutaraldehyde in aqueous solution occurs especially quickly under alkaline pH conditions to yield an unsaturated product (Figure 3.6) [Monsan et al., 1975]. However, glutaraldehyde polymeric moieties exist in aqueous solution as low as pH 5. The order of reactivity of glutaraldehyde with certain compounds is as follows: primary amines > peptides > guanidines > secondary amines > hydroxyl groups. Compared with other aldehydes such as formaldehyde, the crosslinks of glutaraldehyde are more stable [Woodroff, 1979].
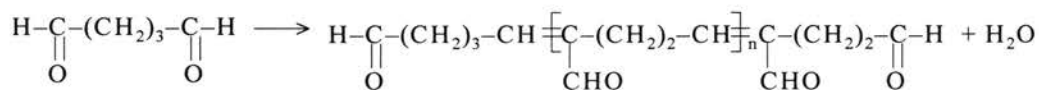
Figure 3.6. Reaction scheme for polymerization of aqueous glutaraldehyde.

Glutaraldehyde, as a crosslinker, is so efficient that it has been clinically used as afixative in bioprostheses and drug delivery matrices since 1969. In the literature, glutaraldehyde also is a common crosslinker employed to link functional molecules to biomaterials in order to improve the haemocompatibility [Amiji and Park, 1993; Bui and Thompson, 1993; Marconi *et al.*, 1996; Seifert *et al.*, 1997]. Since the applications of glutaraldehyde as a crosslinker have been very successful, glutaraldehyde is utilized in the following experiments.

3.4 Experimental Methods

Reagents. Polyethylene telephthalate films (PET, Malinex) and medical grade polyurethane beads (PU, Tecoflex SG-93A) were generously provided by DuPont Polyester Films (Hepewell, VA) and Thermedics Inc (Woburn, MA), respectively. Phosphate buffered saline 10 × (PBS, pH 7.4) was obtained from Life Technologies (Gaithersburg, MD). Tetrahydrofuran (THF) and toluene were purchased from Fisher Scientific (Fairlawn, NJ). 5-Iodoacetamidofluorescein (5-IAF), a specific fluorescent labeling agent for thiols, was purchased from Pierce (Rockford, IL). L-cysteine, glycine, glutaraldehyde (GA) (50%), ethylenediamine, 3-aminopropyltriethoxysilane (APTES), and all other chemicals were purchased from Sigma Chemicals (St. Louis, MO).

Immobilization of L-cysteine and glycine onto PET and PU surface. Primary amino groups were attached onto the PET film surface as previously described [Desai and Hubbell, 1991]. Briefly, PET films were immersed in acetone for more than 24 hr to remove most physically adsorbed contaminants. The films were then incubated in 50% (v/v) aqueous ethylenediamine for 24 hrs at 40 °C to incorporate a primary amine at the

PET ester linkage. The aminated PET films were then rinsed with deionized water, dried, and were ready for activation with glutaraldehyde.

Polyurethane (PU) films were made by dissolving PU beads in THF at 60 °C at a concentration of 10 % (w/v) and casting in a $10 \times 6 \times 0.4$ cm^3 pit within an aluminum plate. The dried PU film was soaked in toluene for 24 hrs at room temperature, and then reacted with 2% (v/v) APTES in toluene under a nitrogen atmosphere for a period of 24 hrs to form an aminated surface. The aminated PU films were washed thoroughly with toluene and cured for at 24 hrs at room temperature prior to modification with glutaraldehyde.

The resulting aminated films (both PET and PU, always freshly aminated) were exposed to GA. This was accomplished by incubating the films in 10 mM phosphate buffer (pH 7.0) containing 1% GA (w/v) and room temperature under a nitrogen atmosphere for 1 hr.

The glutaraldehyde-activated films were then rinsed with 1× PBS buffer to eliminate the excess of unreacted glutaraldehyde and then immediately transferred into a 0.2% (w/v) L-cysteine in 10 mM phosphate buffer (pH 7.0) at room temperature for at least 3 hrs. The coupling condition of pH 7.0 was employed in order to stabilize the imine bond (-C=N-). Glycine, a non-thiol amino acid, was similarly coupled to separate PET and PU polymer surfaces as a control. All modified polymers were washed with excess water prior to further testing. The entire immobilization procedures are summarized in Figure 3.7.

Qualitative detection of immobilized L-cysteine using fluorescent labeling. First, the principle underlying this fluorescent labeling is briefly described. Fluorescent

66

50% Ethylenediamine
————————————→
40 °C, 24 hrs

(PET)

-NH-(CH$_2$)$_2$-NH$_2$

2% APTES in toluene
————————————→
24 hrs, under nitrogen

(PU)

>Si-(CH$_2$)$_3$-NH$_2$

1% Glutaraldehyde
————————————→
pH 7, 1 hr, under nitrogen

-N=CH-(CH$_2$)$_3$-CHO

(GA-modified Polymer)

0.2% L-Cysteine
————————————→
pH 7, 3 hrs

-N=CH-(CH$_2$)$_3$-C=N-Cys

(L-cysteine-modified Polymer)

0.2% Glycine
————————————→
pH 7, 3 hrs

-N=CH-(CH$_2$)$_3$-C=N-Gly

(Glycine-modified Polymer)
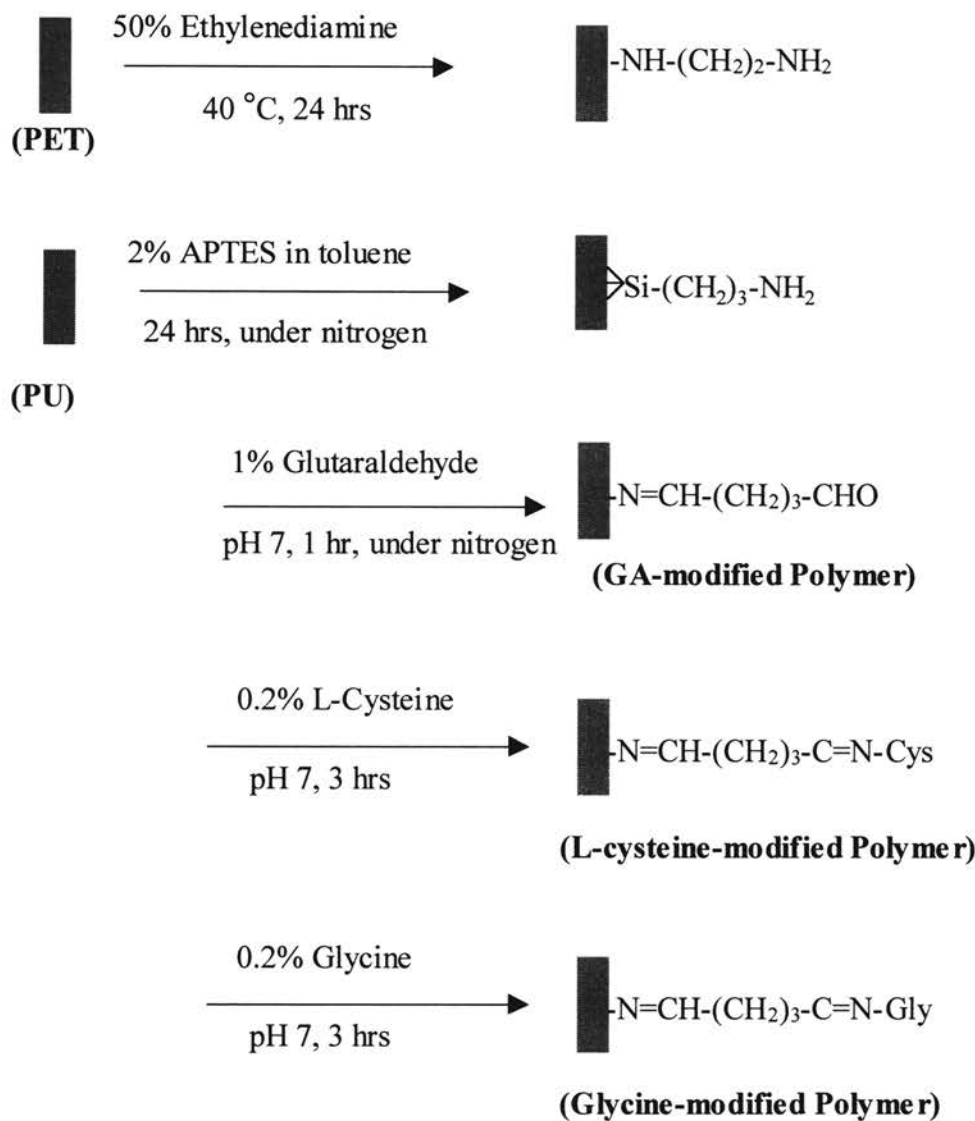
Figure 3.7. Reaction schemes of immobilizing L-cysteine and glycine onto the surface of polyethylene terephthalate (PET) and polyurethane (PU) using glutaraldehyde as a crosslinker. APTES is 3-aminopropyltriethoxysilane.

labeling is widely used in cell sorting, histochemistry, molecular structure and function studies, and many other experimental techniques for attaching highly sensitive visual and spectrophotometric markers to substances for identification and observation. For this study, a fluorescent dye (5-IAF) was selected to qualitatively determine whether L-cysteine was attached on both polymers since 5-IAF specifically reacts with the thiol group derived from cysteine.

When a fluorescent molecule (e.g., 5-IAF) is irradiated with energy (light) of an appropriate wavelength called the excitation spectrum (EX_{max}), a portion of this energy is absorbed and an electron is excited to a higher energy state. As the electron returns to its ground (unexcited) state, they do so in a series of steps or cascades. The energy associated with these electronic transitions is released and emitted as visible light usually within a certain range of wavelength called the emission spectrum (EM_{max}). The spectral characteristics of 5-IAP are EX_{max} 490-495 nm and EM_{max} 515-520 nm.

A fluorometer is usually required to view the specific light emitted from the fluorescent dyes attached on the functional molecules. The basic components of a fluorescence microscope include an excitation light source, wavelength selection devices (filters), objectives, detectors, stages, and camera [Herman, 1998]. For the desirable detection of light emitted from a fluorescent reagent, two things are noteworthy: (i) the short pass filter (SP) must match the EX_{max} of the fluorescent dye so that the light passed through the filter can be absorbed; (ii) the long pass filter (LP) should match the EM_{max} of the fluorescent reagent to allow emitted light to pass through to the detector. For this study, an epi-fluorescence illumination microscope was used (EFP-3, Nikon Corporation, Melville, NY) and the excitation light source was a xenon lamp.

The protocol for fluorescent labeling L-cysteine immobilized on polyurethane and PET and detection with the fluorescence microscope is illustrated as follows.

- ~2 mg 5-IAF was dissolved in 2 ml 50 mM phosphate buffer (pH7.0). 5-IAF is soluble in aqueous solution at above pH 6. The solution should be prepared freshly since the fluorescence intensity fades when it is placed in solution (50% lost within 32 days due to storage) [Valnes and Brandtzaeg, 1985].

- 1 cm^2 freshly prepared L-cysteine-modified PET or polyurethane was rinsed with deionized water and transferred to a 2.5 ml microcentrifuge tube. Then, 1 ml 5-IAF solution prepared as above was added. Here freshly prepared L-cysteine-modified polymer was used because 5-IAF does not react with any disulfide (oxidized L-cysteine).

- The microcentrifuge tube was incubated in the dark for 1 hr at ambient temperature to complete the reaction of 5-IAF with the thiol group of immobilized L-cysteine.

- At the same time, 1 cm^2 glycine-modified polyurethane or PET was similarly incubated in another 1 ml 5-IAF solution as a control.

- After incubation, both L-cysteine-modified and glycine-modified polymers were washed several times to remove unreacted 5-IAF and detected separately with the fluorescence microscope at 400 ×.

3.5 Results and discussion

In all cases, fluorescence was only observed with both of the L-cysteine-modified polymers, which means that free thiol groups existed on the L-cysteine-modified polymer and not on the glycine-modified polymer. This assay qualitatively demonstrated that L-cysteine was successfully immobilized onto polyurethane and PET. In the next chapter, a quantitative assay will be described to precisely determine the amount of L-cysteine immobilized onto both polymers.

A probable reaction scheme for the aminolysis of PET with ethylenediamine is illustrated in Figure3.8. One of the amino groups in ethylenediamine can insert into the ester bond in the PET polymer and the other amino group remains for further reaction with glutaraldehyde.

$$[-O-CH_2-CH_2-O-\underset{O}{\overset{||}{C}}-\bigcirc-\underset{O}{\overset{||}{C}}-]_n \ + \ H_2N-(CH_2)_2-NH_2$$

$$\xrightarrow[40\,°C]{24\ hr} \ [-O-CH_2-CH_2-OH \ \ HN-\underset{O}{\overset{||}{C}}-\bigcirc-\underset{O}{\overset{||}{C}}-]_n$$
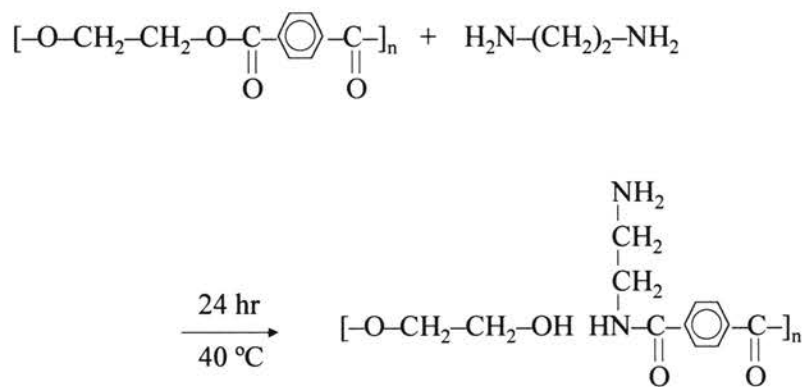
Figure 3.8. The chemical reaction to aminate PET with ethylenediamine.

The specific reaction between polyurethane and APTES (a silane) remains to be identified. At least two possible reactions may contribute to the silylated surface, which is discussed as follows.

70

Silanes have been widely used to modify glass, silicon, quartz surfaces, and many metal oxide surfaces, which are all rich in hydroxyl groups [Plueddemann, 1980]. A wide range of different silanes are available, permitting many different chemical functional groups to be incorporated on surfaces (Table 3.1). The advantages of silane reactions are their stability, which is due to their covalent, cross-linked structure. A typical silane surface modification reaction is proposed in Figure 3.9 [Rafter and Hoffman, 1996].

Table 3.1 Silanes for Surface Modification of Biomaterials

$$X - \underset{\underset{X}{|}}{\overset{\overset{X}{|}}{Si}} - R$$

X = leaving group	R= functional group
—Cl	—$(CH_2)_nCH_3$
—OCH_3	—$(CH_2)_3NH_2$
—OCH_2CH_3	—$(CH_2)_2(CF_2)_5CF_3$
	—$(CH_2)_3O\text{-}CO\text{-}C(CH_3)\text{=}CH_2$
	—$(CH_2)_2$– ⬡

APTES: $X = -OCH_2CH_3$ $R = -(CH_2)_3NH_2$

The end groups of polyurethane are hydroxyl (-OH), which can react with ethoxy groups of APTES and initialize the silanization according to the reaction scheme depicted in Figure 3.9. APTES can be tied into the silane film network without reaction with hydroxyl group on the surface of the polymer although APTES is not directly bound to the surface. Another explanation for the reaction between APTES and polyurethane is that traces of adsorbed surface water can trigger the polymerization of silane to form
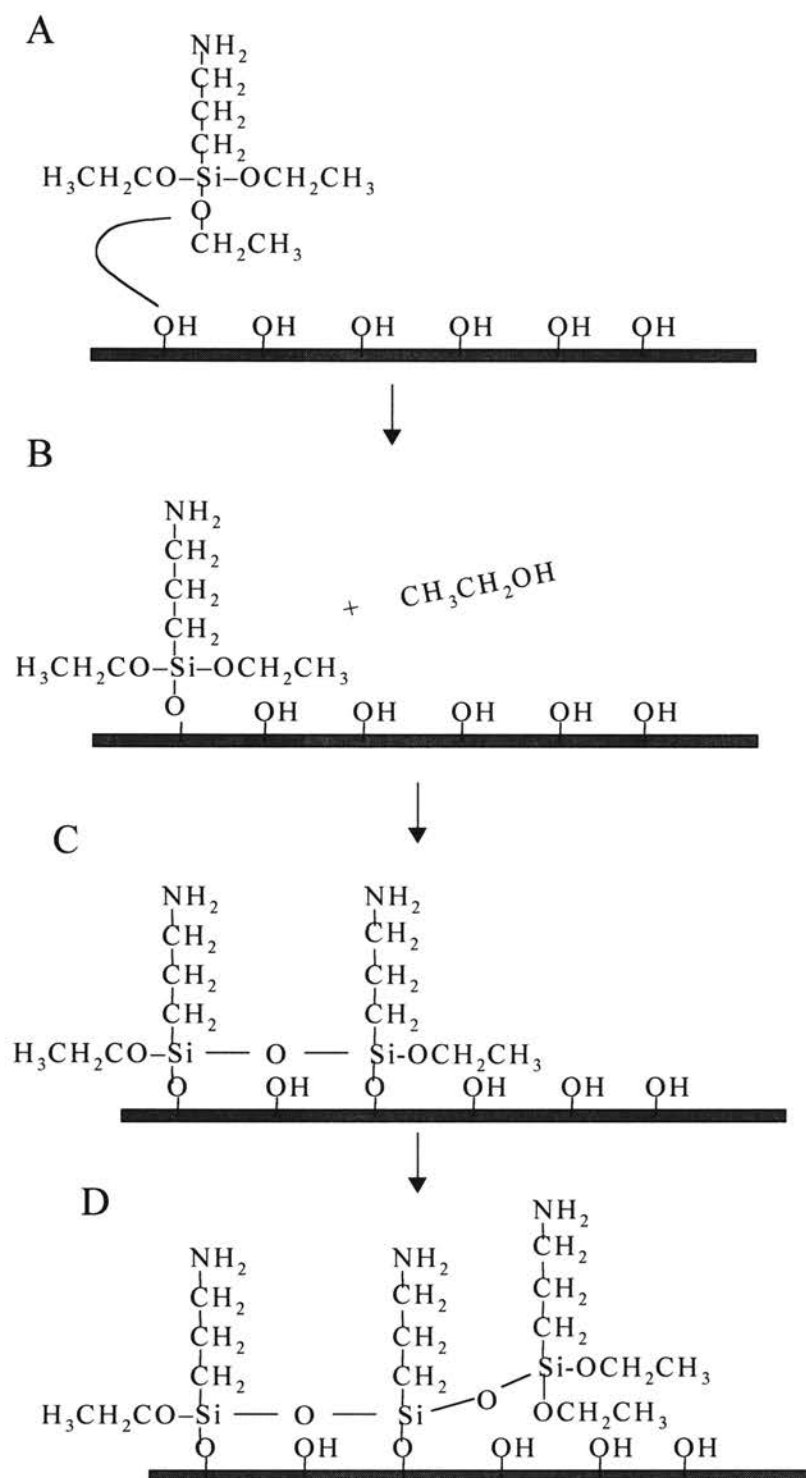
Figure 3.9. The chemistry of a typical silane surface modification. A) A hydroxylated surface is exposed to APTES (3-aminopropyltriethoxysilane). B) One ethoxy group couples with a hydroxyl group, releasing ethanol. C) Two ethoxy groups of another APTES react with a surface hydroxyl group and an ethoxy group from the first attached APTES. D) The process continues with further APTES. Figure modified from Ratner and Hoffman, 1996.

polysiloxane, a structure similar to that shown in Figure 3.9. In both cases, the R group of APTES ($-(CH_2)_3NH_2$) is left and the end amino group can easily react with glutaraldehyde to form a Schiff's base.

It is worthy noting about the toxicity of glutaraldehyde since the modified polymer is designed for applications involving human subjects. Several studies have reported on the adverse biological response to glutaraldehyde-treated bioprostheses and tissue [Makkes *et al.*, 1978; Speer *et al.*, 1980; Chvapil *et al.*, 1983; Beauchamp et al., 1992]. Residual glutaraldehyde remaining in the bioprostheses, as well as unstable glutaraldehyde polymers, have been implicated in inflammatroy reactions, cytotoxicity, fibrosis, and calcification [Schoen *et al.*, 1988; Tsai *et al.*, 2001]. The results of the studies about glutaraldehyde toxicity have been conflicting [Jayakrishnan and Jameela, 1996]. Those investigators who reported the adverse effects of glutaraldehyde generally employed a higher concentration compared with those who found that glutaraldehyde treatment did not affect biological performance [Ketharnathan and Christie, 1980; Cooke et al., 1983]. McPherson et al. (1986) examined the influence of initial glutaraldehyde treatment concentration on the biological response to injectable fibrillar collagen implants and showed that the biological response to the implants correlated with the concentration of glutaraldehyde used for crosslinking.

In addition, thorough rinsing of the crosslinked tissue has been found to eliminate the cytotoxic effects of glutaraldehyde, suggesting that complete removal or inactivation of the remaining aldehyde should ensure that the implant is not cytotoxic. Gendler et al. (1984) investigated the optimum time required for adequately rinsing the bioprostheses in order to eliminate the cytotoxic effects of glutaraldehyde, which was monitored in mice

and in cell culture. Extracts of pericardial tissue washed three times in normal saline for 10 min after glutaraldehyde fixation in 1% solution showed no toxicity. Treatment with glycine was also reported to reduce the toxicity to some extent [Jayakrishnan and Jameela, 1996]. Chvapil et al. (1987) cross-linked bovine pericardium using glutaraldehyde under various temperature, pH, and time conditions and found that cytotoxicity of glutaraldehyde could be eliminated. Therefore, the detrimental effects of glutaraldehyde could be removed or at least alleviated if sufficient care was exercised.

In these studies, L-cysteine is also a very small molecule compared with protein and should be able to quench all the aldehyde groups on the polymer after the aminated polymers react with glutaraldehyde. Thus, L-cysteine immobilization itself can attenuate or eliminate the potential toxicity of glutaraldehyde-activated polymers.

CHAPTER 4

CHEMILUMINESCENCE-BASED ASSAY OF L-CYSTEINE

In the last chapter, the experimental protocol for covalently immobilizing L-cysteine to PET and polyurethane was elaborated. A fluorescence-labeling assay qualitatively showed that the immobilization of L-cysteine via chemical reaction was successful. Here, a chemiluminescence-based assay for quantifying immobilized L-cysteine is described for determining the amount of L-cysteine immobilized on PET and polyurethane. This method employs nitrosation of L-cysteine in the presence of equal or excess nitrite under acidic conditions. Following nitrosation, nitrosated L-cysteine in the solution and any remaining nitrite can be converted to NO in a reducing reagent modified with free iodine and free L-cysteine, respectively, for analysis. Although the development of this assay was originally motivated for quantifying immobilized L-cysteine, it can also be applied for determining free L-cysteine in biological media.

4.1 Previous methods for quantifying L-cysteine

L-cysteine plays an important role in physiological systems including (i) ameliorating heavy metal toxicity [Baker *et al.*, 1987; Quig, 1998], (ii) regulating the nitrogen balance and body cell mass [Droge and Holm 1997; Droge *et al,* 1998], (iii) controlling glutathione and taurine synthesis, and (iv) being a critical substrate and active

site for proteins [Kleinman and Richie, 2000]. S-nitroso-cysteine (Cys-NO), a nitrosated form of L-cysteine, also takes part in several key physiological activities involving endogenous nitric oxide [Myers *et al.*, 1990; Kukreja *et al.*, 1993]. Levels of human plasma thiols, of which free L-cysteine is the primary low molecular weight thiol, are considered as potential indicators of disease and health status [Mansoor *et al.*, 1992; Kleinman and Richie, 2000]. On the other hand, immobilized L-cysteine on solid substrates is used for affinity chromatography and enzyme immobilization [Tyllianakis et al., 1994) as well as for the improvement of the biocompatibility of existing biomaterials [Bui and Thompson, 1993]. L-cysteine as a biomolecule is so important that a variety of analytical methods have been reported to measure L-cysteine in biological media.

Ellman's Assay. Ellman's reagent, 5,5-dithiobis (2-nitrobenzoic acid) (DTNB), reacts with a free thiol group and produces a mixed disulfide and thiolate anion (TNB), of which the latter has a strong spectrophotometric absorbance [Ellman, 1959]. The chemical reaction is illustrated in Eq. 4.1. This approach is widely employed as a routine assay for quantifying thiol groups in biological systems [Riddles *et al.*, 1983; Jocelyn, 1987]. The disadvantages of this assay include thiol autoxication of TNB, a relatively low extinction coefficient value ($\varepsilon_m = 13.7$ mM^{-1}cm^{-1}), sensitivity to pH, and interference with oxygen, nucleophiles, and nitric oxide (NO) donors [Riddles *et al.*, 1983; Gergel and Cederbaum, 1997].

$$\text{RS}^- \; + \; \underset{\text{-OOC}}{\overset{\text{O}_2\text{N}-}{\bigcirc}}\!\!-\text{S-S-}\!\!\underset{\text{COO}^-}{\overset{}{\bigcirc}}\!\!-\text{NO}_2 \; \longrightarrow \; \text{R-S-S-}\!\!\underset{\text{COO}^-}{\overset{}{\bigcirc}}\!\!-\text{NO}_2 \; + \; \underset{\text{-OOC}}{\overset{\text{O}_2\text{N}-}{\bigcirc}}\!\!-\text{S}^- \qquad (4.1)$$

$$\qquad\qquad\qquad\quad \text{DTNB} \qquad\qquad\qquad\qquad\qquad\qquad \text{TNB}$$
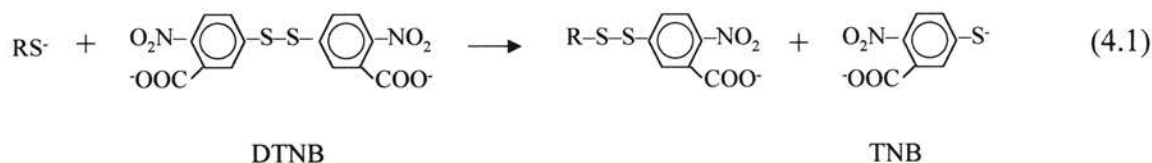
BSA assay. Tyllianakis et al. (1994) published another spectrophotometric assay for the measurement of free thiol groups on solid substrates that overcomes steric hindrance effects of Ellman's reagent. The method utilizes bicinchoninic acid (BCA) to form a chelate complex with Cu^+ that is quantified via spectrophotometry. The complex forms after Cu^{2+} is reduced to Cu^+ by the thiol group (Eq 4.2).

$$2RS^- + 2Cu^{2+} \longrightarrow RS\text{-}SR + 2Cu^+ \qquad (4.2)$$
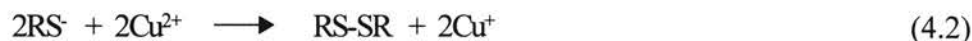
On solid supports, the thiol group is more accessible to the small Cu^{2+} ion as compared with the large Ellman's reagent. In the literature, the experimental data showed that this method was more sensitive than Ellman's assay. Therefore, this assay was used as control to evaluate the chemiluminescence-based assay during quantifying L-cysteine immobilized on agarose gel. However, color contribution may result from any other reducing group with a redox potential lower than Cu^{2+} (such as aldehydo, hydrazido, and NHS esters). Thus, the interference of other species and an inherent lack of sensitivity are still problematic for this method.

Saville's assay. A third spectrophotometric method for quantifying thiols is based on nitrosation, in which a thiol is completely converted into a nitrosothiol via excess nitrous acid [Saville, 1958]. The remaining nitrous acid is removed with ammonium sulfamate (Eq. 4.3). Following the addition of the nitrosothiol to a buffer solution containing mercuric ion, an equivalent of nitrite (NO_2^-) is produced (Eq. 4.4). The released nitrite reacts with sulphanilamide (aromatic amine) to yield the corresponding diazonium salt (Eq. 4.5), which couples with N-1-naphthylethylenediamine to form an intensely coloured azo dye for colorimetric assay. In comparison to Ellman's reagent,

this assay has a higher sensitivity (ε_m=50.0 mM^{-1}cm^{-1}) and overcomes some of the interference with other species. However, potential side reactions and release of nitrite (or nitrous acid) bound to other groups may reduce the accuracy and precision [Jocelyn, 1987]. Although other analytical reagents and mechanisms have also been reported for spectrophotometric measurement of cysteine and thiol groups [Ohmori et al., 1983; Jocelyn, 1987; el-branshy and al-Ghannam, 1995], all these colorimetric methods are not often applicable for measuring L-cysteine in a wide variety of biological media because of low sensitivities.

$$RSH \; + \; HONO \; \longrightarrow \; RSNO \; + \; H_2O \qquad (4.3)$$
$$\downarrow NH_4SO_3NH_2$$
$$NH_4HSO_4 + N_2 + H_2O$$

$$RSNO \; + \; Hg^{2+} + H_2O \; \longrightarrow \; HONO \; + \; RS\text{-}Hg^+ + H^+ \qquad (4.4)$$

$$HONO \; + \; ArNH_2 + H^+ \; \longrightarrow \; ArN^+{\equiv}N \; + \; 2H_2O \qquad (4.5)$$
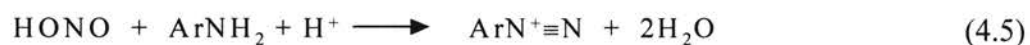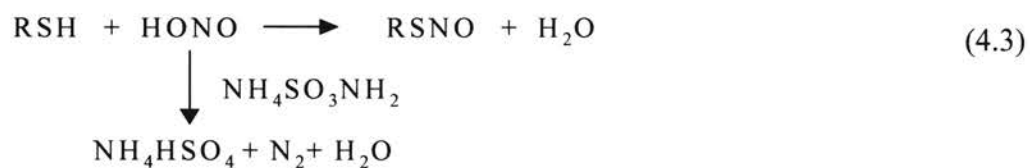
Recently, thiols have also been quantified via fluorescence or electrochemical detection [Richie and Lang, 1987; Mansoor *et al.*,1992; Tsikas *et al.*, 1998; Ivanov *et al.*, 2000]. Although the selectivity and sensitivity of these thiol assays have been dramatically improved compared to the previously described spectrophometric methods, and are useful for assaying biological samples, none of these methods have been utilized for quantifying L-cysteine immobilized on solid substrates.

4.2 Theoretical basis for the chemiluminescence-based assay

The purpose of this study was directed toward the development of a sensitive analytical method applicable for measuring free as well as immobilized L-cysteine, which is mainly based on the following three research facts:

a) Low molecular weight thiols such as L-cysteine and glutathione can be completely nitrosated by equimolar or excess nitrous acid in less than 30 minutes [Byler *et al.*, 1983; Keaney *et al.*, 1993; Meyer *et al.*, 1994]. Liu *et al.* (1994) also reported that no free thiol on agarose gel was detected after exposed to NO_2^- in 0.5 M HCl as a result of nitrosation, which means that immobilized L-cysteine also can be nitrosated at the same condition.

b) NO moieties in nitrite and S-nitroso-glutathione (GSNO) can be released and the release can be managed by using different reducing reagents. Samouilov and Zweier (1998) showed that nitrite or GSNO can release all their NO moieties as a form of NO when a sample containing nitrite and GSNO was added to a reducing reagent (1% KI in 1M HCl) containing excess I_2. However, NO release from GSNO was almost completely suppressed and only nitrite can release NO when the sample was added into the reducing reagent containing excess L-cysteine. Their co-workers developed a assay to quantify GSNO in the sample containing nitrite and GSNO according to this observation since NO released in the aqueous solution can be measured with several available methods.

c) A chemiluminescence NO analyzer has been intensively employed to precisely measure NO in the liquid phase, which is based on a

chemiluminescence reaction between NO and ozone [Cox, 1980]. It has been one of the primary tools for detecting NO and its derivative (e.g., S-nitrosothiols) [Stamler et al., 1992; Alpert et al., 1997; Samouilov and Zweier, 1998;] since NO was recognized as a key messenger biomolecule involving many physiological activities in the later 1980s. At the optimized conditions, the sensitivity of the NO analyzer can be down to as low as 1 nM [Marlery et al., 2000].

Therefore, we proposed that NO release from S-nitroso-L-cysteine (CySNO) and nitrite could be controlled as similar GSNO and nitrite using two different reducing reagents after free or immobilized L-cysteine in the sample is completely converted into (CySNO) via excess acidified nitrite. Then CySNO, equal to the initial L-cysteine, can be calculated according to the amount of NO measured via a chemiluminescence NO analyzer. The following experiments support this proposal.

4.3 Materials and methods.

Reagents. Sodium nitrite, glacial acetic acid, and potassium iodide were purchased from Fisher Scientific (Fairlawn, NJ). Phosphate buffered saline (PBS, pH7.4) was obtained from Life Technologies (Gaithersburg, MD). L-cysteine agarose, L-cysteine, bovine serum albumin (BSA), iodine, and all the other reagents were purchased from Sigma Chemical Co. (St. Louis, MO). L-cysteine-modified PET (PET-Cys) and L-cysteine-modified polyurethane (PU-Cys) was freshly prepared according to the protocol described in Chapter 3.

Nitrosation of free and immobilized L-cysteine. Free L-cysteine, (PET-Cys), PU-Cys, and L-cysteine agarose were nitrosated via acidified NO_2^-, which is a typical method for nitrosating thiols (Meyer et al., 1994; Samouilov and Zweier, 1998). Excess NO_2^- was generally used to ensure complete nitrosation. For free L-cysteine, 2 μM NO_2^- was added to a 1 ml solution containing 1 to 4 μM L-cysteine in 0.5 M HCl (excess and equimolar L-cysteine concentrations were used in some cases to consume all the NO_2^-). PET-Cys or PU-Cys was freshly prepared and cut into small pieces (1 cm x 1 cm). Each piece was added to a 0.5 M HCl solution (1 ml) initially containing 40 μM NO_2^-. Prior to nitrosation, L-cysteine agarose was incubated in 1mM dithiolthreitol for 5 min and then rinsed with water, with centrifugation following each step. L-cysteine agarose (0.2 ml) was then added to 1 ml of 0.5 M HCl initially containing 200 μM NO_2^-. Larger amounts of NO_2^- were used in the nitrosation of the immobilized L-cysteine due to larger sampling sizes required as a result of handling constraints.

During nitrosation, the solutions were gently shaken for 30 min (nitrosation of PET-Cys and PU-Cys took 60 min to completely detach immobilized L-cysteine as discussed later). Aqueous samples were taken at the designed time (for agarose, the gel was separated from the sample via centrifugation). All samples were neutralized with an equal volume of 0.5 M NaOH and stored on ice prior to analysis to maintain the stability of any Cys-NO in the sample. All nitrosation procedures were carried out in capped micro-centrifuge tubes to prevent NO from escaping from the system. In addition to nitrosation of the L-cysteine samples, purified nitrosated BSA (BSANO) was similarly obtained by adding excess NO_2^- (in 0.5 M HCl) and then desalting the solution through a

Sephadex G-25 column which will be described in detail in Chapter 5. BSANO was used for assessing the L-cysteine analytical method.

Release of NO from nitrosated immobilized L-cysteine. 0.4 ml agarose L-cysteine, 1 cm^2 PET-Cys, and 1 cm^2 PU-Cys were nitrosated via acidified nitrite as above. After nitrosation, agarose gel was washed three times with deionized water to remove the remaining nitrite. Centrifugation was employed to separate agarose gel from aqueous phase after each step. Nitrosated agarose gel (0.2) was added to each of two 10 ml tubes, one containing 5 ml 10 mM PBS and the other with 40 μM cupric sulfate in 5 ml 10 mM PBS. Nitrosated PET-Cys and PU-Cys were simply rinsed with water and then gently cleaned. Then the two films were then transferred into separate 2.5 ml micro-centrifuge tube with 1 ml 10 mM PBS containing 40 μM cupric sulfate. Aqueous samples were taken at intervals from all the tubes which were continuously shaken. The amount of nitrite in the samples was detected using the following chemiluminescence NO analyzer via the reducing reagent consisting of 2.5 ml KI and 7.5 ml glacial acid.

Chemiluminescence Analysis. A Sievers 270B chemiluminescence NO analyzer (Seivers Corporation, Boulder, CO) was used to measure the NO released in the solution in order to measure the amount of nitrosated thiols and NO_2^- in each sample. Total nitrosated thiol and NO_2^- were measured via a reducing solution consisting of 0.2 M potassium iodide (2.5 ml) saturated with iodine (I_2) and 7.5 ml glacial acetic acid. The reducing solution promotes NO release from both NO_2^- and nitrosothiols for detection. NO_2^- alone was measured via a similar reducing solution containing no I_2, but supplemented with 25 mM L-cysteine. Additional L-cysteine has been shown to suppress NO release from GSNO [Samouilov and Zweier, 1998], such that similar effects

were expected for CySNO. The nitrosothiol concentration was obtained by the difference between NO released from the total nitrosated thiols plus NO_2^- and NO from NO_2^- alone after the amount of NO was measured using the two modified reducing reagents.

The experimental setup for detecting NO release from the aqueous solution is schematically depicted in Figure 4.1. After the appropriate reducing solution was added to a continuously purged vial (D × H: 20mm × 70mm) using nitrogen and a fritted disk (Pore Diameter: 25-50 μm), the solution was purged for several minutes until a stable detector pressure was reached with no background signal. Aqueous samples were drawn from the nitrosation studies with a gas-tight syringe (Hamilton Company, Reno, NV) and injected into the reducing solution. The NO released from the sample was carried with the nitrogen into the reaction cell, in which NO reacted with ozone (O_3) to yield a signal proportional to the amount of NO released from the purging vial. Thus, using a proper calibrant, the amount of NO released in the reducing solution was quantified. In this study, NO_2^- was employed as the calibrant since NO_2^- is completely converted into NO in both reducing solutions. The volume of each sample varied between 20 and 200 μl depending on the recorded signal. Additionally, an acid trap immersed in an ice bath was added to condense and remove glacial acid vapors from the nitrogen stream.

Comparison method. Immobilized L-cysteine on both PET and agarose was also determined by the BCA assay for comparison. The BCA method is reported to be more accurate than Ellman's method for quantifying thiol groups immobilized onto solid substrates because of steric hindrance to Ellman's reagent [Tyllianakis et al., 1994]. Briefly, a BCA working solution was prepared by mixing 50 parts of solution A (1% BCA, 2% $Na_2CO_3 \cdot H_2O$, 0.16% sodium tartrate, 0.4% NaOH, and 0.95% $NaHCO_3$) and 1
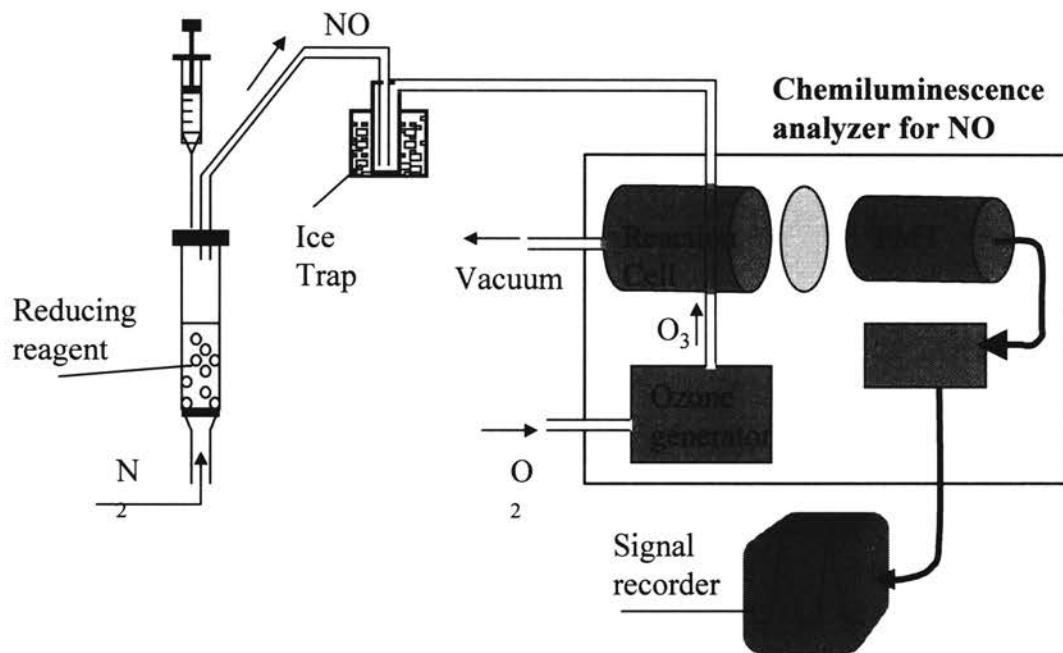
Figure 4.1. Schematic diagram of the instrumental setup for detecting NO released in the reducing solution.

part of solution B (4% CuSO4 ·5H$_2$O) prior to use. The solid samples containing immobilized L-cysteine were incubated in 2.0 ml of the BCA working solution at 60 °C for 1 hr. The amount of L-cysteine on the solid substrate was estimated by measuring the absorbance of the liquid phase at 562 nm. Standards for calibration consisted of free L-cysteine.

4.4 Results

Analysis of NO$_2^-$ and Cys-NO. The chemiluminescence signals of NO$_2^-$ standards in both free iodine and L-cysteine modified reducing reagents are shown in Figure 4.2. Although linear signals were observed in both cases, the signal level of NO$_2^-$ was ~12% lower in the presence of L-cysteine as compared with that in the presence of free iodine. The phenomenon that L-cysteine diminished total conversion of NO$_2^-$ to NO at low pH was also reported by Robak et al. (1997). Thus, different NO$_2^-$ calibration curves were used depending on the reducing solution.

The detection limit for NO$_2^-$ was as low as 0.02 nmol per injection, which corresponds to 0.1 μM if a 0.2 ml sample was injected. The intra-assay variability was less than 2% and the inter-assay variability was less than 5%. Each time samples were analyzed at a significant time following the previous calibration, a corresponding NO$_2^-$ calibration curve was established in order to minimize any inter-assay error. In this study, the detector signal (representing the peak height), instead of the signal area, was used for the calibration. The linearity and the same width for each peak signal showed that this simplification was applicable.
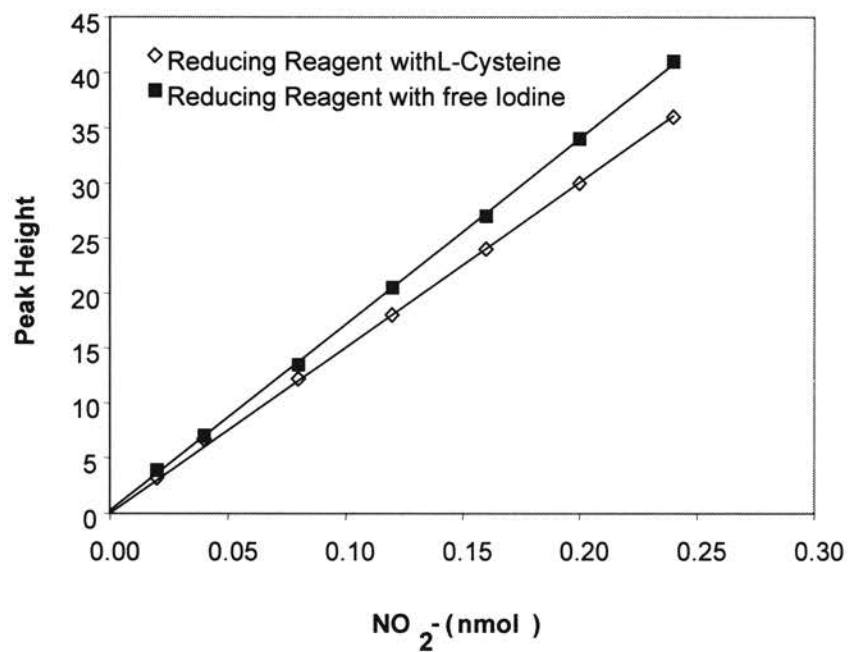
Figure 4.2. Linearity of chemiluminescence nitric oxide analyzer of detecting NO release from NO_2^- in the modified reducing reagents. R^2 = 0.9994 for L-cysteine added, and R^2 = 0.9998 for free iodine added.

In order to derive CySNO in the sample containing NO_2^- and CySNO via NO measurement, NO release from NO_2^- and CySNO was first evaluated in the reducing solution with free iodine. When equimolar NO_2^-, CySNO, or an equimolar mixture of the two was injected into the reducing reagent containing free iodine, the same signal was recorded for each sample as shown in Figure 4.3. Thus, the kinetics of NO release from NO_2^- and Cys-NO are very similar in the free-iodine reducing environment. Therefore, the total NO moieties in the sample containing CySNO and NO_2^- can be quantified using a NO_2^- calibration curve based upon the free-iodine reducing reagent.

Figure 4.4 shows the signal for similar amounts of NO_2^- and CySNO added to the L-cysteine modified reducing solution. As is evident, 90% of NO release from Cys-NO was suppressed and NO release from BSA-NO was essentially completely blocked when L-cysteine was added to the reducing reagent. The most unstable nitrosothiol, Cys-NO, cannot be totally blocked by L-cysteine with regards to NO release although L-cysteine is effective in stabilizing nitrosothiols such as BSA-NO and GSNO [Samouilov and Zweier, 1998]. The detector signal of 0.50 nmol Cys-NO was double that of 0.25 nmol Cys-NO, which showed that NO release from Cys-NO was linear despite a 90% suppression in the signal.

From the above observations, the detector signal represents 100% NO_2^- and 100% Cys-NO when the free-iodine modified reducing solution is employed (denoted as $(NO)_{iodine}$). Similarly, the signal represents 100% NO_2^- and 10% Cys-NO in the L-cysteine modified reducing solution (denoted as $(NO)_{L-cysteine}$). Thus, the concentration of Cys-NO in a sample is calculated as Eq. 4.6
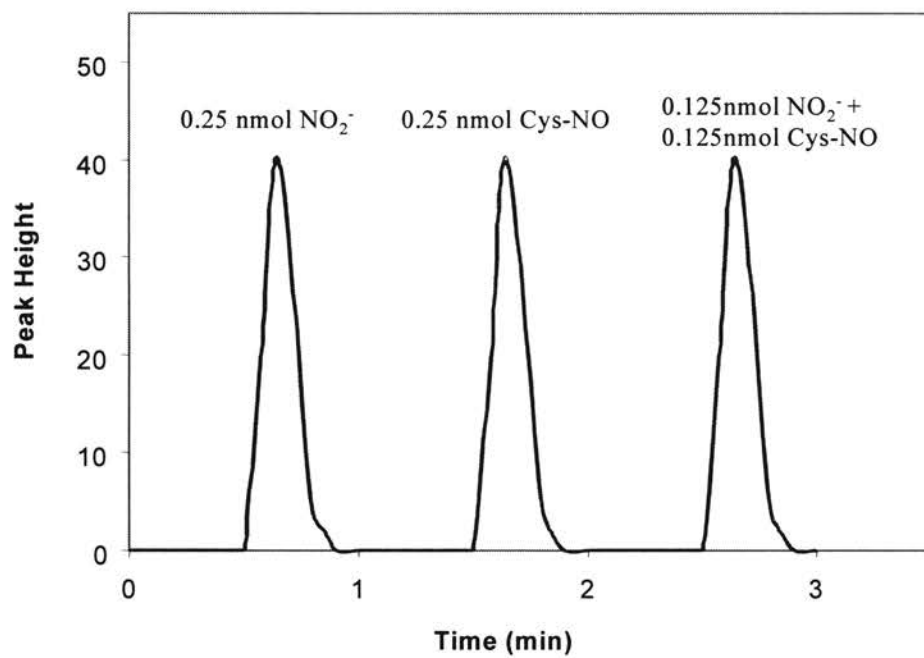
Figure 4.3. Chemiluminescence signal from NO2-, CySNO, and a mixture of both in the presence of a reducing reagent modified with free iodine.
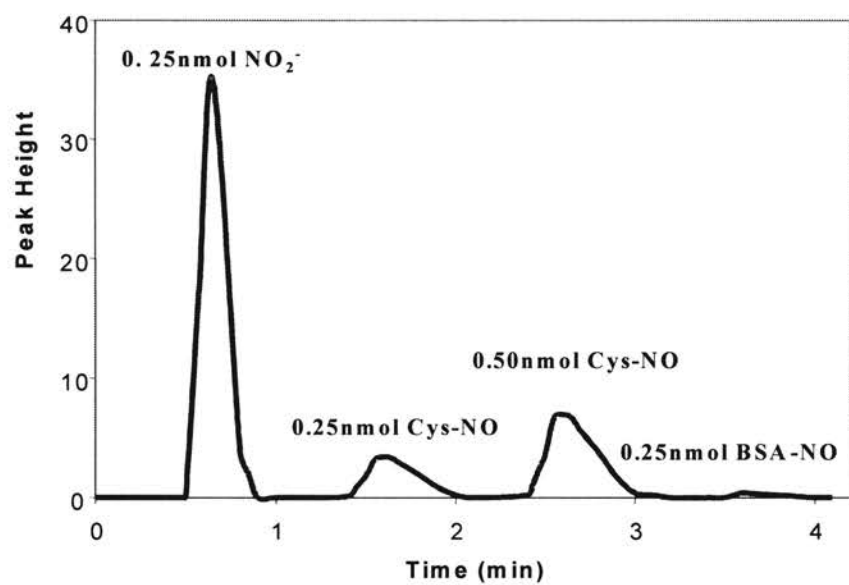
Figure 4.4. Chemiluminescence signal from NO2-, CySNO, and BSANO in the presence of a reducing reagent modified with L-cysteine.

$$(CySNO) = [(NO)_{iodine} - (NO)_{L\text{-}cysteine}] / 0.90 \qquad (4.6)$$

The validity of Eq.4.6 was evaluated by quantifying the amount of Cys-NO produced after nitrosation where different ratios of L-cysteine to NO_2^- were added (Table 4.1). Since nitrosation of L-cysteine by NO_2^- at acidic conditions essentially goes to completion, all L-cysteine would be converted into CySNO in the presence of excess NO_2^-. Thus, the measured Cys-NO should be equal to the L-cysteine added. Similarly, the measured Cys-NO should be equal to the NO_2^- added when excess L-cysteine is added. The results in Table 4.1 are in a excellent agreement with the above statements. The error between measured and theoretical L-cysteine and NO_2^- is less than 4% and the standard deviation is less than 2%. Therefore, free L-cysteine in aqueous solution, in the absence of interfering thiols, can be quantified using excess NO_2^- during nitrosation according to Eq. 4.6.

Analysis of immobilized L-cysteine. L-cysteine agarose was nitrosated by acidic NO_2^- and, after rinsing, was transferred into an aqueous solution containing cupric ion, which promotes the release of NO from nitrosated thiols (as see in Figure 4.5). In the absence of cupric ion (10 mM PBS buffer may contain trace of cupric ion due to contamination), nitrosated agarose was relatively stable. However, in the presence of 40 μM cupric ion, NO released from the agarose gel within 3 hr was more than half of the amount of original L-cysteine. These results shows that nitrosated L-cysteine stayed on the gel after nitrosation, and the covalent bond between L-cysteine and agarose is relatively stable and can withstand acidic conditions during nitrosation.

TABLE 4.1

CySNO determined from nitrosation of different ratios of initial L-cysteine and NO_2^-

	NO_2^- added	L-Cysteine added	$(NO)_{iodine}$	$(NO)_{L\text{-}cysteine}$	Cys-NO[a]
1	2.00	1.00	1.98 ± 0.04	1.09 ± 0.03	0.99 ± 0.03
2	2.00	1.50	2.03 ± 0.01	0.70 ± 0.03	1.47 ± 0.04
3	2.00	4.00	2.00 ± 0.01	0.22 ± 0.01	1.98 ± 0.01

Note. The units are μM. The values are expressed as Mean value ± AD (n=2).
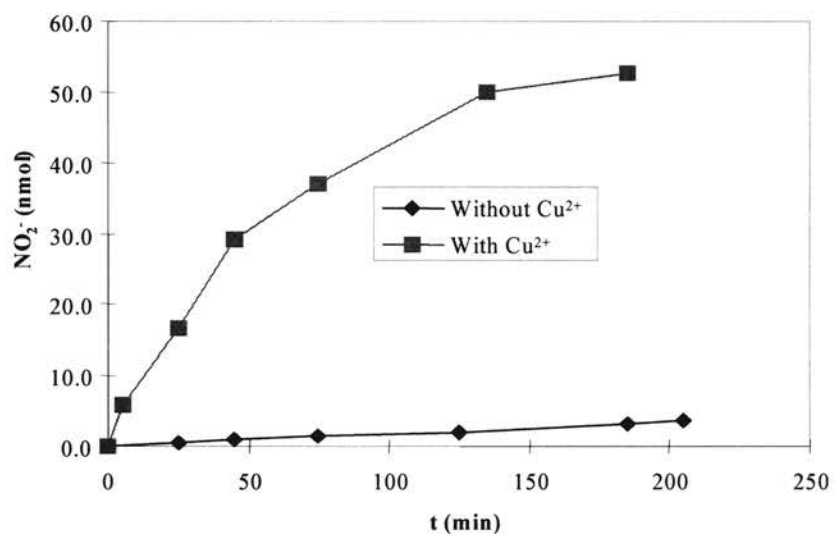[a] Cys-NO was derived according to Eq.4.6.

Figure 4.5. The NO release profile of 0.2 ml nitrosated agarose L-cysteine in 10 mM PBS buffer. 40 μM cupric sulfate present in the aqueous phase strongly enhanced NO release.

Since the bond connecting L-cysteine to agarose is stable and nitrosation was carried out in capped micro-centrifuge tubes to eliminate NO loss, the L-cysteine amount on the gel can be quantified by the difference of NO_2^- in the liquid phase between the initial and end of the nitrosation process. The simplified mechanism is depicted in Figure 4.6. NO_2^- in the solution was determined using the free-iodine modified reducing reagent. The results showed 0.54 ± 0.05 (n=3) μmol L-cysteine per ml of agarose. In comparison, the BCA method gave a value of 0.53 ± 0.06 (n=3), demonstrating excellent agreement. The standard curve obtained by the BCA assay using L-cystiene is indicated in Figure 4.7. As compared with the value provided by the manufacturer (0.64), the measured L-cysteine was in general agreement. The slight discrepancies may be due to storage and sample preparation.

Table 4.2

Determination of the amount of L-cysteine on agarose

This assay	BCA assay	Manuf. value
0.54 ± 0.04	0.53 ± 0.06	0.64

Unit: μmol/ml gel. Values are Mean ± SD (n=3).

The same experimental protocol was performed to quantify the amount of L-cysteine immobilized on PET and polyurethane. The calculated value of L-cysteine was very low and highly variable from batch-to-batch (data not shown). When nitrosated PET-Cys was incubated in 10 mM PBS buffer containing 40 μM cupric sulfate, nitrite

93

A
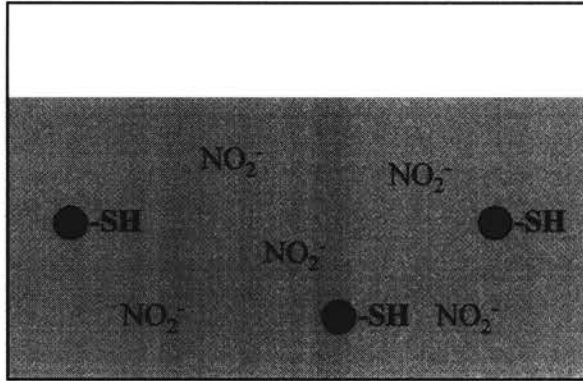
At the initial nitrosation, the system contains 5 nitrite and 3 L-cysteine on agarose gel.

B
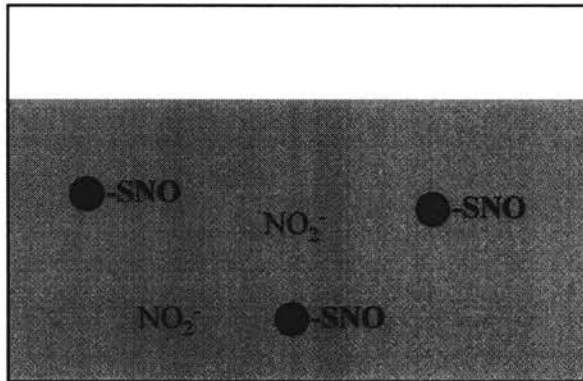
After complete nitrosation, the system contains 2 nitrite and 3 nitrosated L-cysteine on agarose gel.

Figure 4.6. Scheme for determining the amount of L-cysteine on agarose gel through measuring nitrite at the beginning and end of nitrosation.

$$y = 0.0228x$$
$$R^2 = 0.9999$$

Figure 4.7. Standard curve used for measuring L-cysteine by the BSA assay.

was not detectable. These observations can be explained by the hypothesis that the imine bond is hydrolyzed during nitrosation (acidic conditions) and no L-cysteine remains on the polymer surface, although the imine bond is stable at neutral pH. Thus, L-cysteine is detached from the polymer surface and nitrosated in the surrounding solution.

Therefore, L-cysteine immobilized on the PET and polyurethane according the protocol in Chapter 3 can be similarly detec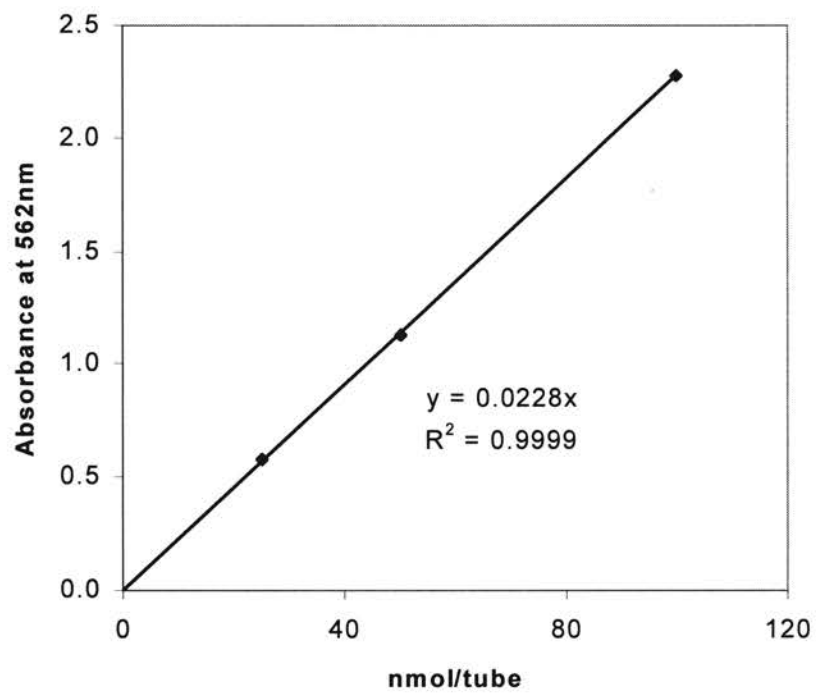ted as free L-cysteine. Owing to the unknown kinetics of the breakage of the imine bond during acidic nitrosation, the surrounding solution was sampled at various time intervals during nitrosation. Sampling analysis was performed in the reducing agent containing free iodine and again in the L-cysteine modified reducing agent to obtain the CySNO concentration according to Eq. 4.6. Approximately 60 minutes was required to reach the steady state value for CySNO analysis in the liquid phase (see Figure 4.8). The calculated value of L-cysteine immobilized on the PET surface and polyurethane were consistently 8.1 ± 1.1 nmol/cm^2 (n=5) and 5.2 ± 0.9 nmol/cm^2 (n=3), respectively.

Comparatively, the range of the value obtained by the BCA assay was widely sporadic for L-cysteine-modified PET (Table 4.3). The standard deviation was more than 60% of the average value (n=3). The values of L-cysteine immobilized on PET (n=3) and PU (n=1) obtained by the BCA assay were more than double and quadruple of the corresponding values by the chemiluminescence-based assay, respectively. Data in Table 4.3 also show that other unknown reducing functional groups on modified PET and polyurethane except L-cysteine can also react with Cu^{2+} to a yield color compound and interfere with the accuracy of this comparison method. Therefore, the BCA assay is not

applicable for quantifying L-cysteine immobilized on PET and polyurethane according to the protocol described in Chapter 3.

Table 4.3

Equivalent L-cysteine on modified PETs and polyurethane obtained by the BCA assay

Sample	PET-GA[a]	PET-Gly[b]	PET-Cys
Equivalent L-cysteine[c] (nmol/cm^2)	7.58 ± 3.60	7.02 ± 5.13	20.60 ± 12.75

Sample	PU-GA	PU-Gly	PU-Cys
Equivalent L-cysteine (nmol/cm^2)	8.43	6.21	24.35

Note: a) -GA means glutaraldehyde attached.
b) -Gly means glycine attached.
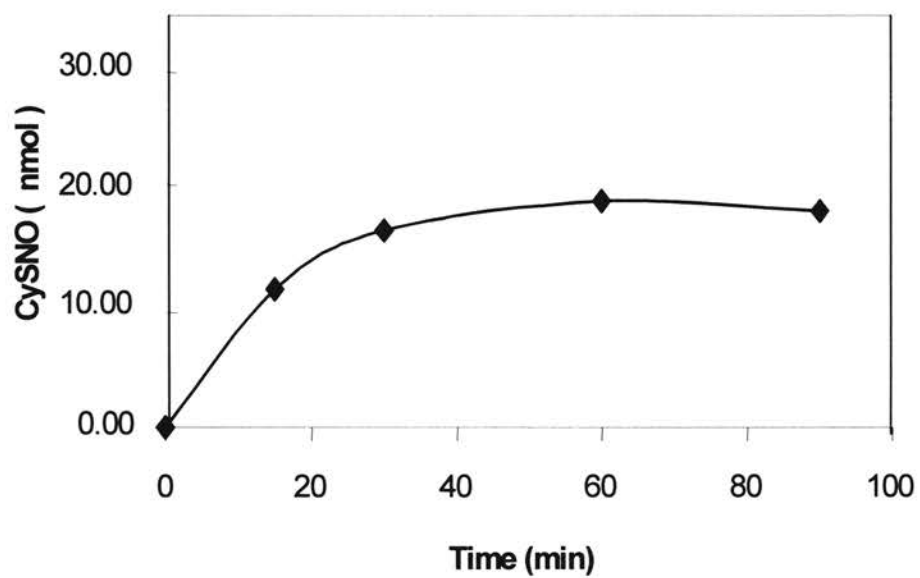c) The value is expressed as Mean Value $\pm$ SD (n=3)

Figure 4.8. The amount of CySNO in the liquid phase as a function of incubation time. 2 cm^2 PET-Cys was immersed in 1 ml 0.5 M HCl containing 40 nmol NO^{2-}. The value of CySNO was calculated using Eq. 4.6.

4.5 Discussion

Free iodine- and L-cysteine-modified reducing reagents. Reaction (Eq. 4.7) used for quantitative reduction of nitrite to NO by the reducing reagent (2.5 ml 0.2 M KI + 7.5 ml glacial acid) also forms free iodine which is soluble in acidified KI solution. During the preparation of the reducing reagent, iodine can also be a product of oxidation of HI by atmospheric oxygen (Eq. 4.8). With the formation of iodine which exists as I_3^- or HI_3, the solution turns brown in color and this phenomenon was observed during preparation. Thus in acidified KI solution, uncontrolled small amount of free iodine yielded which can slowly catalyze NO release from S-nitrosothiols [Samouilov and Zweier, 1998].

$$2HNO_2 + 2HI \longrightarrow 2NO + I_2 + 2H_2O \qquad (4.7)$$

$$O_2 + 4HI \longrightarrow 2 I_2 + 2H_2O \qquad (4.8)$$
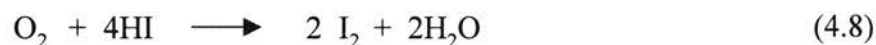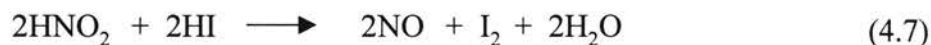
Addition of excess free iodine to the acidic solution of KI causes rapid stoichiometric release of NO from nitrosothiols as illustrated by Eqs. 4.9-4.12. I_3^- reacts with RSNO as an oxidizing agent producing thiol radical and nitrosoium ion (Eq. 4.10). Thiol radicals recombine and produce disulfides (Eq. 4.11), while nitrosonium is reduced to NO by potassium iodide (Eq. 4.12). This is a catalytic redox cycle for I_2 which is dependent on the presence of additional of reducing equivalents (I^-). The presence of free iodine does not alter the rate and the yield of NO from nitrite reduction (Figure 4.3). Thus, acidified KI solution containing free iodine results in quantitative conversion of nitrite to NO as well as quantitative release from nitrosothiols.

$$I_2 + I^- \longrightarrow I_3^- \tag{4.9}$$

$$I_3^- + 2RSNO \longrightarrow 3I^- + 2RS^{\cdot} + 2NO^+ \tag{4.10}$$

$$2RS^{\cdot} \longrightarrow RS\text{-}SR \tag{4.11}$$

$$2NO^+ + 2I^- \longrightarrow 2NO + I_2 \tag{4.12}$$

Free iodine has mild oxidative properties and can be reduced to I^- by the addition of reducing agents. During the preparation of the reducing reagent (2.5 ml 0.2 M KI + 7.5 ml glacial acid) containing 25 mM L-cysteine, disappearance of the brownish tint occurred immediately after addition of these reducing agents to KI solution, indicating that iodine was consumed as

$$2RSH + I_2 \longrightarrow RS\text{-}SR + 2HI \tag{4.13}$$

The added L-cysteine blocked the rapid production of NO from nitrosothiols (Figure 4.4 and Eq. 4.10). One possible reason is that the removal of iodine quenches the iodine catalyzed process; The other is that excess L-cysteine present has been observed to have a function of stabilizing nitrosothiols [Feelisch *et al.,* 1994; Pietraforte *et al.,* 1996; Robak, 1997] although a small amount of L-cysteine can catalyze NO release from S-nitrosothiols. However, the addition of L-cysteine into the reducing reagent did not inhibit the slow spontaneous release of NO from the self-decomposition of nitrosothiols [Samouilov and Zweier, 1998]. This may well explain that addition of excess L-cysteine to the reducing reagent can almost completely suppress NO release from BSANO and GSNO can almost completely be suppressed, and not from CySNO because BSANO and GSNO is much more stable than CySNO.

Evaluation of the chemiluminescence-based assay. In this study, a chemiluminescence-based method was presented which can be used for detection of free and immobilized L-cysteine. As shown in Figure 4.2, 0.02 nmol NO_2^- or CySNO can easily be measured at the lower detection limit. Although this sensitivity is not completely optimized, the detection limit is very sensitive for the measurement of physiological levels of free L-cysteine and biologically used immobilized L-cysteine. In contrast, the BSA assay, another method specific for determining L-cysteine on solid substrates, has a detection limit of 0.9 nmol per sample of immobilized L-cysteine [Tyllianakis et al., 1994]. The extinction coefficient of Saville' assay is about three times of that of Ellman's reagent. However, the limit of quantitation of the Saville's assay is also only down to ~1 nmol per sample [Jocelyn, 1987]. Therefore, the method described in this work has a sensitivity of more than an order of magnitude of the reported spectrophotometric methods.

Selectivity is also an impressive feature of this methodology. Addition of free iodine to the reducing reagent is used to catalyze spontaneous release NO from nitrosated L-cysteine as previously described [Samouilov and Zweier, 1998]. Addition of L-cysteine to the reducing reagent is used to scavenge free iodine produced from oxidation of I^- in the reducing agent and block catalytic release of NO from CySNO by free iodine. Also excess L-cysteine can substantially slow the self-decomposition of nitrosothiols as well as slightly suppress NO release from NO_2^- [Pietraforte, 1995; Robak, 1997]

One specific limitation should be emphasized for the developed assay. Similar to other chemiluminescence-based nitrosothiol assays [Alpert et al., 1997; Samouilov and Zweier,1998], this method cannot distinguish between different nitrosothiols. However,

the incorporation of HPLC or other chromatographic separation systems makes it possible to separate thiols [Tsikas et al., 1999] so that this method could then be used for quantifying each thiol.

Overall, free L-cysteine and immobilized L-cysteine can be sensitively and accurately quantified using the described methods. For immobilized L-cysteine, the assay works whether the covalent bond connecting L-cysteine to the solid substrate is stable or susceptible to breakage by a strong acid. Compared with spectrophotometric assays for L-cysteine, this method is more sensitive and specific. This methodology should be valuable for studies of free L-cysteine, Cys-NO, and L-cysteine on solid substrates in biological systems.

L-cysteine concentration on PET and polyurethane. In the experimental results, the amount of immobilized L-cysteine was about 8 nmol/cm^2 for PET and 5 nmol/cm^2 for polyurethane if a single layer of thiol groups are formed on the polymer, the maximal theoretical value can be calculated according to the equation

$$Conc \ (nmol \ / \ cm^2) = \frac{1}{\pi \ r^2 N_A} \tag{4.14}$$

where r is the radius of thiol group (cm), N_A is Avogadro constant (6.023×10^{14} nmol^{-1}). If the value of r is designated as the sum of the radii of a hydrogen and a sulfur atoms, then r is 1.34×10^{-10} m (the well-known diameter of H$_2$O is 3.5×10^{-10} m) according to Table 4.4. Thus, the maximal single layer coverage of L-cysteine on the polymer surface is ~3 nmol/cm^2, which is much less than the value measured by the chemiluminescence-based assay. In fact, the value of r should be the radius of the molecule L-cysteine

instead of that of the thiol group and some free space should exist among immobilized L-cysteine. Therefore, the theoretical value should be also less than ~3 nmol/cm^2.

Table 4.4

Covalent Radii for some Atoms *

Atom	Radius (10^{-10} m)	
	single bond	double bond
H	0.30	
C	0.772	0.667
O	0.66	0.55
S	0.104	

* Data from Dean Eds. Lang's Handbook of Chemistry, p4.23

The possible explanation is that polymerized glutaraldehyde is attached onto the aminated PET and polyurethane since the reactions are carried out at pH 7.0 and room temperature, in which the polymerization of glutaraldehyde can occur (see Figure 3.6). Once polymerized glutaraldehyde is attached onto the aminated PET or PU, multiple L-cysteine can be immobilized onto in a single polymerized glutaraldehyde via the reaction of aldehyde group with the primary amino group. In this case, multiple layers of L-cysteine, instead of a single layer, can be attached on the polymer surface. Therefore, the concentration of immobilized L-cysteine on both PET and PU can be more than the maximal theoretical value of a single layer. This phenomenon obviously has to be explored.

CHAPTER 5

EVIDENCE FOR THE MECHANISM USING ENDOGENOUS NO

As described in Chapter 2, the core of this thesis is to demonstrate that immobilized L-cysteine can extract NO from abundant S-nitrosoproteins in blood and then generate localized NO release to improve the haemocompatibility of blood-contacting polymers. This novel concept may eventually overcome the disadvantages of NO-releasing polymers. The specific protocol was described to immobilize L-cysteine onto two pivotal biomaterials PET and polyurethane (in Chapter 3). Both a qualitative assay (fluorescent labeling) in Chapter 3 and a quantitative assay (chemiluminescence-based assay developed in this thesis and the BCA assay) in Chapter 4 demonstrated that the modification was successful.

In this chapter, L-cysteine-modified PET and polyurethane are employed as substrates to prove the mechanism: (i) L-cysteine-modified biomaterials are not favorable for platelet adhesion only in the presence of blood plasma, which infers that NO may be transferred to immobilized L-cysteine from S-nitroso-proteins in plasma and then released to inhibit platelet adhesion; (ii) L-cysteine modified biomaterials, instead of glycine-modified biomaterials (control), extracts NO from S-nitroso-proteins via its thiol group when exposed to an aqueous solution containing S-nitroso-proteins (called transnitrosation); (iii) NO transferred to the L-cysteine-modified polymer is released during transnitrosation due to the instability of CySNO. All these points are

demonstrated in the experiments described later. In the experiments of transnitrosation, nitrosated bovine serum albumin (BSANO) was utilized since it has similar NO-releasing properties as nitrosated human serum albumin (AlbSNO) [Scorza et al., 1997] and is also relatively less expensive. Thus, purification of BSANO using gel filtration will be presented to remove nitrite and other salt after BSANO is synthesized via excess nitrite under the acidic conditions.

5.1 Desalting nitrosated bovine serum albumin using gel filtration

Gel filtration is also known as molecular sieving, gel permeation and size exclusion chromatography (SEC). It has been used as a biotechnological process for the purification of enzymes, polysaccharides, nucleic acids, proteins and other biological macromolecules for decades. Gel filtration materials are very stable because of their ineptness towards biomolecules. In the experimental laboratory, gel filtration is reliable and simple, little equipment is required, the procedures are straightforward, and good separations and high yields are usually obtained.

5.1.1 General concepts and principles of gel filtration

Important terminology used in gel filtration. V_t is the total volume of eluent (mobile phase) inside and outside of the beads. The unhydrated gel matrix frequently occupies as little as 1% of the total volume of the column so the volume of the gel bed usually is considered as V_t. The volume of gel is referred to as the bed volume or column volume, which is composed of the space occupied by the gel beads V_x, and the space

occupied by the solvent surrounding the gel beads, which is also referred to as the void volume, V_o. Therefore,

$$V_t = V_x + V_o \qquad\qquad (5.1)$$

The void volume is roughly estimated to be one-third of the bed volume [Rosenberg, 1996]. A molecule that is too large to enter the pores of the column matrix is said to be excluded and is eluted from the column in the void volume. The exclusion limit of a particular gel is the molecular weight of the smallest molecule that cannot enter the gel. The elution volume of a particular solute (V_e) is expressed as the amount of effluent solution exiting from the column between the time that the solute first penetrates the gel bed to the time that it appears in the effluent. V_e is usually measured from the maximal peak height appearing in the effluent stream (Absorbance at 280 nm for separating protein). The distribution coefficient K_D, which is equal to

$$K_D = (V_e - V_o) / (V_t - V_o) \qquad\qquad (5.2)$$

is a useful value for the calculation of the molecular weight of a protein when gel filtration is used as an analytical tool to determine the molecular weight (Rosenberg, 1996].

Mechanism of separation via gel filtration. Gel filtration separate molecules according to differences in their size as they pass through a column packed with a gel. The gel, which is in bead form for easy column packing, consists of an open, cross-linked three-dimensional molecular network of pores into which molecules of less than maximum pore size may penetrate. The pores within the beads are of such sizes that some are not accessible to large molecules, but small molecules can penetrate all pores. The large molecules (above the molecular weight exclusion limit) will not be readily

106

retained in the column and are eluted by the volume of the eluent (mobile phase) equal to the void volume of the column V_o. This means that the elution volume V_e equals V_o ($V_e = V_o$). The small molecules with the sizes that are compatible with size of eluent molecules permeate all pores of gel and diffuse back into the mobile phase. The consequence of this repeated process is that the elution volume equals the total volume ($V_e = V_t = V_o + V_x$).

Any specific grade of a gel matrix has a certain proportion of pores that are accessible to the molecules of intermediate dimensions. Such molecules, which can enter the pores large enough to accommodate them, move back into eluent, and are eluted from the column with an elution volume of

$$V_e = V_o + K_D V_t \tag{5.3}$$

Each specific size of molecule has a different K_D ranging from 0 to 1. The larger the size of the molecule, the smaller the value of K_D. Consequently, molecules are eluted in order of their decreasing size (Figure 5.1).
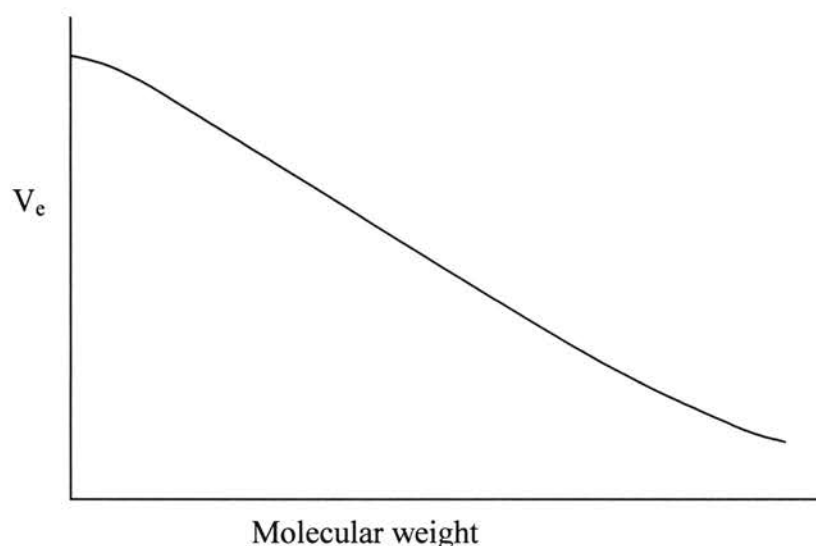

Figure 5.1. A typical plot of the log (mol wt) of molecules versus the elution volume V_e obtained from gel filtration.

In this study, gel filtration was employed to desalt BSANO after exposure of BSA with acidified nitrite. The molecular weight of BSA is 66.4 kDa. Nitrite and chloride ions, which are intended to be removed, have the molecular weight of less than 100 Da. Thus Sephadex G-25, which is dextran homogeneously crosslinked with epichlorhydrine and has a exclusion limit of 5000 Da, was selected as the gel matrix since it is effective in desalting proteins [Rosenberg, 1996]. Another advantage of Sephadex G-25 is its relative hardness, which allows the beads to resist distortion and stand higher pressure, generating good flow characteristics and fast effluent flow rate. In the literature, it was reported that Sephadex G-25 column was used to purify BSANO [Meyer *et al.,* 1994; Hogg, 1999]. For this study, Sephadex G-25 was purchased form Sigma Chemicals (St. Louis, MO).

5.1.2 Experimental materials and procedures

Nitrosation of BSA. 0.24 ml 4.0 mM BSA was added to a capped micro-centrifuge tube containing 0.12 ml 10 mM nitrite and 0.12 ml 1.0 M HCl. The tube was gently shaken for 50 min to allow for nitrosation of BSA. In previous studies (Chapter 4), all nitrosation was carried out at acidified conditions as high as 0.5 M HCl. Here, the final concentration of HCl was 0.25 M during nitrosation since BSA can be denatured and become adhesive at 0.5 M. The nitrosation time was increased from 30 min to 50 min in consideration of the reduced concentration of HCl. Excess acidified nitrite was added to ensure complete nitrosation of BSA.

Separation via gel filtration. The experimental setup for gel filtration is relatively simple (Figure 5.2), consisting of a gel column, pump, and fraction collector. In this experiment, the eluent (water or 20 mM PBS buffer) was directly pumped through